International Journal of Nanomedicine

Dovepress
Taylor & Francis Group

Open Access Full Text Article

ORIGINAL RESEARCH

Triphenylphosphonium Bolaamphiphile-Liposomes Loaded with Resveratrol and Trolox: Mitochondriotropic Formulations with Therapeutic Potential in Neurodegeneration and Cancer

Francesca Ceccacci[1,*], Fabrizio Ciranna[2,*], Simona Sennato[3], Beatrice Simonis[1], Alessia Ciogli[4], Stefano Gallina[2], Sofia Migani[5,6], Annarica Calcabrini[5], Riccardo Salvio[1,7], Eleonora Calicchia[2], Giuseppina Bozzuto[5], Viviana Moresi[8], Cecilia Bombelli[1]

[1]Institute for Biological Systems (ISB)-CNR, Secondary Office of Rome-Reaction Mechanisms c/o Department of Chemistry, Sapienza University, Rome, Italy; [2]Department of Chemistry, Sapienza University, Rome, Italy; [3]Institute for Complex Systems (ISC)-CNR and Physics Department Sapienza University, Rome, Italy; [4]Department of Drug Chemistry and Technology, Sapienza University, Rome, Italy; [5]National Centre for Drug Research and Evaluation, National Institute of Health, Rome, Italy; [6]School of Science and Technology, Chemistry Unit, University of Camerino, Camerino, Macerata, Italy; [7]Department of Chemical Science and Technology, Tor Vergata University, Rome, Italy; [8]Institute of Nanotechnology (NANOTEC)-CNR, c/o Sapienza University of Rome, Rome, Italy

*These authors contributed equally to this work

Correspondence: Simona Sennato; Giuseppina Bozzuto, Email simona.sennato@cnr.it; giuseppina.bozzuto@iss.it

Purpose: We aimed to develop mitochondriotropic liposomes (TPP3-liposomes) formulated with a phospholipid (PC) and the triphenylphosphonium bolaamphiphile TPP3, and encapsulate two antioxidants, trans-resveratrol (hydrophobic) and Trolox (hydrophilic), for mitochondrial therapy of neurodegeneration and drug-resistant tumors.

Methods: The influence of the PC (saturated or unsaturated) and TPP3/PC ratio on liposome physico-chemical properties (diameter, polydispersity, charge, transition temperature, and stability over time) were investigated by Dynamic and Dielectrophoretic Light Scattering measurements. Evaluation of cytotoxicity, mitochondrial targeting and effect on mitochondrial membrane potential of TPP3-liposomes were conducted utilizing an MTT assay, laser scanning confocal microscopy and flow cytometry on drug-resistant human breast cancer cells (MDA-MB231) and murine skeletal muscle cells (C2C12): MDA-MB231 cells have been selected as a model for studying multiple drug resistance (MDR) in cancer; C2C12 cells have been chosen to investigate the oxidative stress associated with the ageing process and neurodegenerative muscle diseases. Two different strategies were explored for antioxidant loading: active loading into the liposome aqueous cavity (resveratrol, Trolox) and passive loading inside the lipid bilayer membrane (resveratrol).

Results: The amount of TPP3 bolaamphiphile and lipid composition affect liposomes' physicochemical properties, liposome bilayer organization, and antioxidant loading efficiency. TPP3 confers the ability to reach mitochondria even in low amounts (2.5%); liposomes with 2.5% of TPP3 are non-toxic and capable of encapsulating the antioxidants. TPP3-liposomes encapsulating trans-resveratrol in the lipid bilayer membrane or in the aqueous cavity were developed, with high entrapment efficiency in both cases. Trolox was encapsulated in the aqueous cavity of liposomes, without precedents in literature, with very high entrapment efficiency and enhanced stability following encapsulation. TPP3-liposomes can deliver resveratrol to the mitochondria in the MDA-MB231 cells, exerting a protective activity on the mitochondrial structure.

Conclusion: Our findings support the potential of antioxidant-loaded liposomes as adjuvants in neurodegenerative diseases or sensitizing agents in cancer therapy.

Keywords: mitochondriotropic liposomes, antioxidants, sensitizing agents, MDR in cancer, neurodegenerative diseases, target therapy

https://doi.org/10.2147/IJN.S539303
Received: 14 June 2025
Accepted: 31 December 2025
Published: 27 March 2026

Graphical Abstract

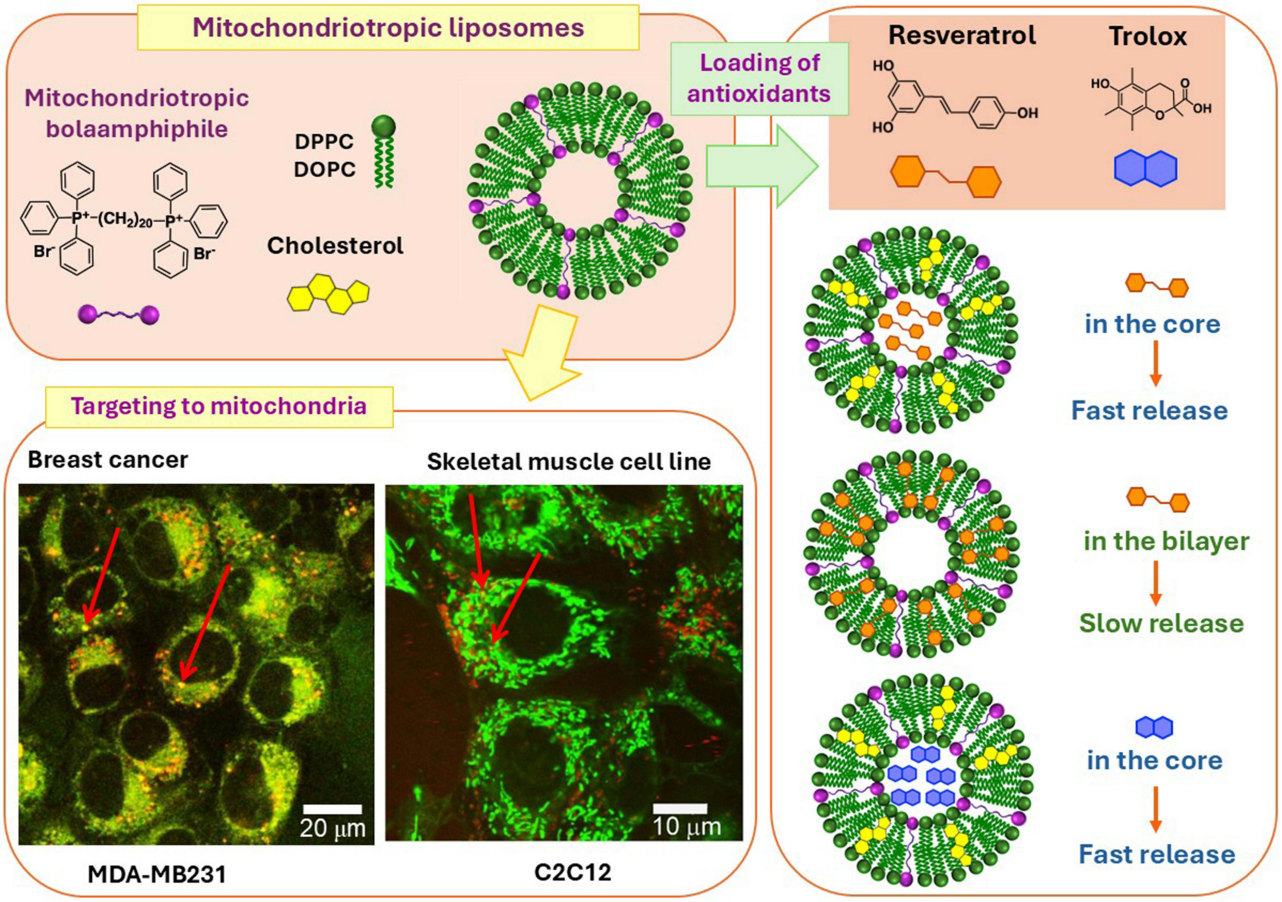

Introduction

Mitochondria play a crucial role in eukaryotic cell life, not only for their energy producing ability but also for their involvement in several vital processes that are essential for maintaining homeostasis and, thus, for cell and whole organism survival. Among the impressive variety of mitochondrial functions, the modulation of ROS levels and the critical role in propagating signals that mediate apoptosis, autophagy, and necrosis are particularly noteworthy in the context of the present work.[1] Given the significant role of mitochondria in the cell cycle, it is not surprising that mitochondrial dysfunction is implicated in many pathologies, such as neurodegenerative and muscle diseases, ischemia-reperfusion injury, diabetes, obesity, cancer, and physiological disorders related to aging. Therefore, with the advent of subcellular targeting, mitochondria have been recognized as promising therapeutic targets for the treatment of several human diseases. Targeting mitochondria is challenging because of the cellular barriers that a drug must cross before reaching the matrix, namely the cell membrane and the two mitochondrial membranes. In particular, the inner membrane is highly convoluted, densely packed, and characterized by a strong negative potential that significantly hinders drug delivery.

Over the years, strategies for targeting mitochondria have been categorized into two main approaches: drug conjugation with mitochondrial-targeting moieties[2] and drug encapsulation in mitochondriotropic nanocarriers, such as liposomes, polymers, and metal particles. Several types of inorganic and organic materials have been investigated for the development of mitochondria-targeting nanocarriers,[3–5] many of which are liposomes or liposome-like vesicles,[6] whose

mitochondriotropic character is bestowed by the presence of octaarginine moieties at high density (MITO-Porter, DF-MITO-Porter), mitochondriotropic peptides[7] or highly delocalized cationic amphiphilic structures, such as the bolaamphiphile dequalinium chloride (DQA) and a variety of triphenylphosphonium (TPP) derivatives. Cationic DQA and TPP-derivatives are driven to mitochondria by the strong negative potential of the inner mitochondrial membrane and can cross the two mitochondrial membranes due to the "soft" nature of their cationic headgroups that are planar structures with highly delocalized cationic charge. Although DQA and TPP derivatives share the same mechanism of action, their mitochondrial targeting efficiency and toxicity can vary significantly depending on the lipid molecular structure, concentration in liposome formulations, and specific cell type.

TPP derivatives have primarily been used in formulation with natural lipids to produce mitochondriotropic nanocarriers[8–12] which, in most cases, show good cell biocompatibility, except for stearyl–TPP based formulations which always show high toxicity.[8] The toxicity of stearyl-TPP derivatives has been mainly attributed to their ability to disrupt the membrane rather than to the depolarization effect resulting from the accumulation of cationic molecules inside the mitochondria.[8] Such results highlight a correlation between the colloidal properties of TPP derivatives and their biological effects.

Some years ago, some of us synthesized a single-chain TPP-bolaamphiphiles, never described in the literature, characterized by two TPP moieties connected by chains of 20 or 30 methylene units, with optimal features for inclusion in liposome formulations.[13,14] These TPP-bolaamphiphiles spontaneously self-assemble into vesicles, which display high stability to dilution and exhibit a coexistence of monomers in an extended and U-shaped conformation within the vesicle layer. The ability to form vesicles, combined with their low detergent character, makes TPP bolaamphiphiles particularly suitable for inclusion in liposomes. Moreover, the extended conformation of the bola can be maintained in liposomes formulated with conventional lipids, resulting in a patchwork membrane composed of monolayer regions formed by the bola and bilayer regions predominantly formed by conventional lipids. This type of membrane organization has two advantages. First, the monolayer region may enhance the capacity of the membrane to retain hydrophilic drugs in the internal aqueous phase. Secondly, the presence of gaps or vacancies at the boundary between the bilayer and monolayer zones may facilitate the hosting and retention of hydrophobic drugs. Most importantly, the TPP moiety should endow liposomes with high specificity for the mitochondria.

Based on the above results, we aimed to develop mitochondriotropic liposomes (TPP3-liposomes) never reported in the literature, formulated with natural phosphocholine (1,2-dipalmitoyl-sn-glycero-3-phosphocholine, DPPC; 1,2-dioleoyl-sn-glycero-3-phosphocholine, DOPC), cholesterol, and the TPP-bolaamphiphile TPP3 which presents a single chain of 20 methylene units (eicosane-1,20-diylbis(triphenylphosphonium) bromide) (Figure 1). We studied the influence of PC (saturated or unsaturated) and the TPP3/PC ratio on the physicochemical properties of the vesicles. We then investigated the ability of selected formulations to target mitochondria in the murine skeletal muscle cell line C2C12 and in the human breast cancer cell line MDA-MB231. Both cell lines represent useful models for investigating different pathological situations, oxidative stress associated with aging and neurodegenerative muscle diseases (C2C12), and multi-drug resistance (MDR) in cancer (MDA-MB231). C2C12 are myoblast cells with excellent ability for growth and differentiation.[15] MDA-MB231 cell line is representative of triple negative breast cancer (TNBC) by showing lack of estrogen and progesterone receptors, absence of HER-2 overexpression/amplification, high heterogeneity and aggressive nature. Furthermore, TNBC is usually poorly differentiated and is often characterized by an MDR phenotype that can be responsible for the high recurrence rates and lack of treatment options.[16] For both the selected cell models (C2C12 and MDA-MB231), mitochondrial delivery could be a good therapeutic strategy, as antioxidants could potentially counteract ROS overproduction and promote cell recovery in neurodegenerative cell models.[6] In addition, selective mitochondrial delivery of anticancer drugs combined with antioxidant molecules could represent a promising strategy to eliminate cancer cells, mainly those displaying a multidrug resistant phenotype, by promoting cell apoptosis from mitochondria.[17]

To evaluate the ability of TPP3-liposome to deliver therapeutics to the mitochondria, we encapsulated two biologically active compounds, trans-resveratrol (RSV) and Trolox. Both RSV and Trolox are good candidates for mitochondrial therapy because of their biological features and antioxidant activity.

Trans-resveratrol is a secondary metabolite produced by a large variety of plants that exerts many therapeutic effects, mostly connected to its ability to modulate three important classes of proteins, ie DNA methyltransferase, histone

 https://doi.org/10.2147/IJN.S539303

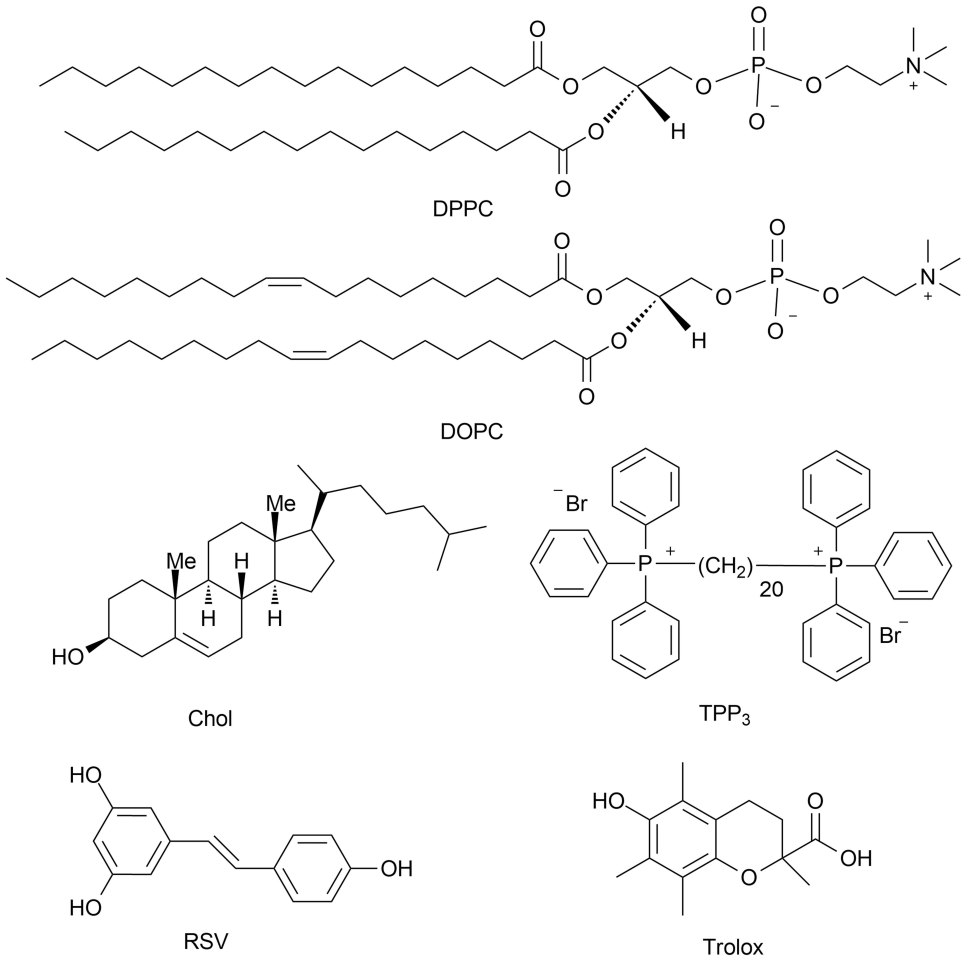

Figure 1 Chemical structures of liposome components and antioxidants.

deacetylase, and lysine-specific demethylase-1.[18] Concerning the chosen cell models, a previous investigation on C2C12 cells reported that RSV can ameliorate muscular dysfunction in-vitro by stimulating myogenesis.[19] Moreover, RSV has been extensively studied for cancer treatment owing to its ability to inhibit three important stages of carcinogenesis: initiation,[20] promotion, and progression.[21] RSV has also been shown to stimulate apoptosis via the mitochondrial apoptotic pathway in retinoblastoma, lung and breast cancer,[22,23] and is an efficient chemosensitizer with limited adverse effects.[24]

Trolox (6-hydroxy-2,5,7,8-tetramethylchroman-2-carboxylic acid) is a soluble synthetic analog of vitamin E that lacks the hydrophobic chain. Trolox is characterized by a very high antioxidant activity and is able to: i) inhibit protein[25–27] and enzyme oxidation;[28–32] ii) prevent the loss of serotonin and dopamine receptors in animal cerebral membranes;[33,34] and iii) protect against different types of cellular damage caused by ROS.[35–39]

In the present study, to develop TPP3-liposomes with high entrapment efficiency and good physicochemical stability, we explored two different loading strategies for antioxidants: active loading into the liposome aqueous cavity and passive loading inside the hydrophobic bilayer membrane. Each strategy involves the use of a tailored lipid matrix for liposome preparation and exploits the specific physicochemical properties of the cargo to be loaded. Indeed, in the active loading protocol, we used liposomes constituted mainly of DPPC and Cholesterol in order to have an impermeable and compact bilayer membrane, and we loaded the antioxidants thanks to the acidic properties of RSV and Trolox; in the passive loading protocol, we exploited the low water solubility of RSV and investigated DPPC and DOPC-based liposomes to evaluate the effect of the different membrane fluidity on the organization of the liposome bilayer membrane and on the

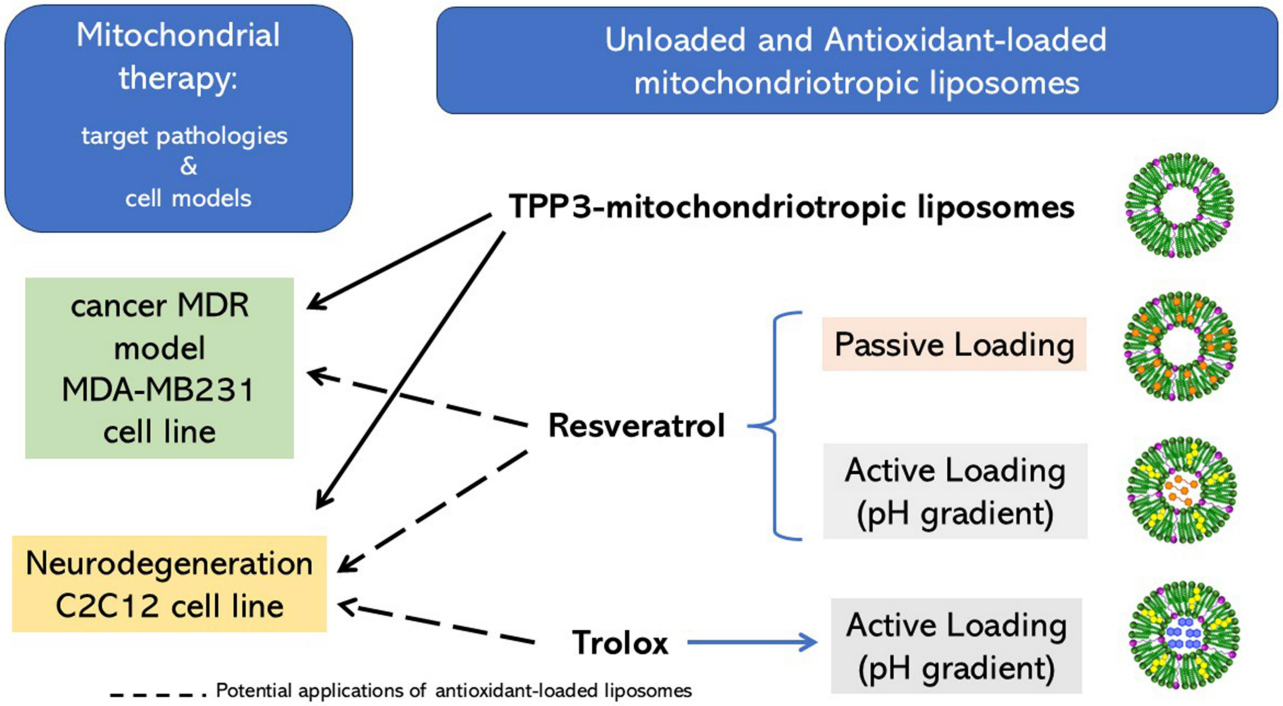

Figure 2 Schematic diagram of the overall content of the investigation, pointing out the content, the objectives, the developed systems and the pathological target.

entrapment efficiency of RSV in the presence of TPP3. Furthermore, we evaluated the ability of TPP3-liposomes to deliver RSV to the mitochondria in MDA-MB231 cells. RSV prevented mitochondrial collapse. The overall strategy of this work is summed up in Figure 2. Our findings highlight the possibility of using liposomal-RSV for the treatment of different diseases, ranging from neurodegeneration to drug-resistant tumors, and to properly modulate its dose.

Materials and Methods

Materials

Phospholipids 1,2-dipalmitoyl-sn-glycero-3-phosphocholine (DPPC), 1,2-dioleoyl-sn-glycero-3-phosphocholine (DOPC), 1,2-dipalmitoyl-sn-glycero-3-phosphoethanolamine-N-(lissamine rhodamine B sulfonyl) (ammonium salt) (16:0 Liss Rhod PE), 1,2-dioleoyl-sn-glycero-3-phosphoethanolamine-N-(lissamine rhodamine B sulfonyl) (ammonium salt) (18:1 Liss Rhod PE) were purchased from Avanti Polar Lipids (Alabaster, AL, USA) and used without further purification (purity > 99%). Bolamphiphile TPP3 was prepared and purified, as previously described.[13,14] Trans-resveratol, Trolox, 8-hydroxypyrene-1,3,6-trisulfonic acid (pyranine), PBS (tablets, final concentration in MilliQ water: 0.01 M phosphate buffer, 0.0027 M KCl, 0.137 M NaCl, pH 7.4, at 25°C), calcium acetate, Sephadex G-50, sodium sulfate, dialysis cellulose membrane (molecular weight cut-off = 14 kDa), MitoTracker probe, 3-(4,5-dimethylthiazol2-yl)-2,5-diphenyltetrazolium bromide (MTT M2128), and solvents were purchased from Sigma-Aldrich. *p*-xylene-bis-pyridinium bromide (DPX) was purchased from Invitrogen (Carlsbad, CA). Dulbecco's Modified Eagle's medium (DMEM), penicillin, streptomycin, L-glutamine, non-essential amino acids, and Fetal Bovine Serum (FBS) were purchased from Euroclone (Pero, MI, Italy).

Preparation of Liposomes

All aqueous solutions were prepared using ultrapure MILLIQ water produced using a Direct-Q3 Millipore apparatus. Aqueous dispersions of the liposomes were prepared according to a previously reported procedure.[40] A lipid film was prepared on the inside wall of a round-bottomed flask by evaporating chloroform solutions containing an appropriate amount of lipids. The film was stored overnight under reduced pressure (0.4 mbar), then hydrated with an appropriate

https://doi.org/10.2147/IJN.S539303

volume of buffer (PBS 150 mM, or calcium acetate 150 mM or 170 mM calcium acetate) and gently warmed above T_M to obtain the desired final lipid concentration. Vigorous lipid shaking using a vortex mixer allowed for the formation of a dispersion of MLVs. MLVs were first freeze-thawed (six times) from liquid nitrogen to a temperature 10°C above the T_M of the liposome formulation and then extruded (10 times) through a 100 nm polycarbonate membrane (Whatman Nucleopore). Extrusions were carried out above the melting temperature using a 2.5 mL or 10 mL extruder (Lipex Biomembranes, Vancouver, Canada).

Liposomes labelled with a fluorescent probe for co-localization experiments with mitochondria were prepared by adding an appropriate volume of the fluorescent probe in chloroform to the lipid mixture, in the step of lipid film preparation (16:0 Rhod-PE for DPPC liposomes and 18:1 Rhod-PE for DOPC liposomes, 0.1% in moles of total lipids).

Characterization of Liposomes: Dynamic and Dielectrophoretic Light Scattering Measurements

Liposome suspensions were investigated using Dynamic and Dielectrophoretic Light Scattering (DLS, DELS) soon after preparation and over 14 days to determine their average diameter, and polydispersity index, ζ-potential and their stability over time and in the presence of Fetal Bovine Serum (FBS). A Malvern Nano-ZetaSizer apparatus equipped with a 5 mW HeNe laser (λ = 632.8 nm) and a backscattering configuration (173°) were used. DLS and DELS measurements were performed at 25°C in triplicate; results represent the average value and the standard deviation.

The cumulant method[41] was used to determine the average hydrodynamic size and the polydispersity index (PDI). For samples with PDI > 0.3, size distribution analysis using the NNLS algorithm[42] was used to ascertain the presence of different populations in the suspension. PALS analysis has been used to measure the electrophoretic mobility and determine the ζ-potential of liposomes.[43]

The thermal phase transition of DPPC/TPP3-liposomes was determined by monitoring the changes in scattered light as a function of temperature,[44] which reflect the modifications of the optical properties of the material, ie the refractive index of the double layer, connected to the phase transition. To obtain the transition temperature T_M, the scattering intensity I (DLS mean count rate) versus the temperature T was fitted using a Boltzmann sigmoid curve.

$$I(T) = \frac{I_2 - I_1}{1 + exp^{(T-T_M)}/\Delta T} + I_2 \quad (1)$$

where I_1 and I_2 are the scattered intensities before and after the observed change, ΔT is the temperature interval at which the transition occurs, and T_M is the temperature at which the intensity, $I(T_M)$, is halfway between the two limiting values, I_1 and I_2. T_M was used as the transition temperature.

Loading of RSV in Liposomes

Lipid composition of liposomal formulations used for loading RSV is indicated in Table 1.

Stability of RSV as a Function of pH and Determination of the First Dissociation Constant

RSV stability as a function of pH was investigated by recording the UV–Vis absorption spectra of a 220 μM solution of RSV in 170 mM calcium acetate at different pH values. Absorption spectra were recorded in the range 250–450 nm in a 1.0 cm path length quartz cuvette on a Cary 300 UV–Vis double-beam spectrophotometer. Except for the measurements, all the samples were kept in the dark.

Potentiometric titrations were performed to assess the first dissociation constant of RSV (Ka_1) for different H_2O/EtOH mixtures using an automatic titrator equipped with a combined microglass pH electrode. The electrode was calibrated for different H_2O/EtOH mixtures (70/30, 60/40, 50/50 v/v) using standard $HClO_4$ and Me_4NOH solutions at different concentrations following the method employed in a previous study for electrode calibration in H_2O/DMSO mixtures.[45–47] The time required to obtain a stable pH reading increased from 1 min in acidic medium to 6 min at a pH above 8.

Potentiometric titrations were performed under a nitrogen atmosphere and in a dark environment using 25 mL of 25 mM RSV solution at 25°C. A 10–50 mM NaOH solution in the same solvent mixture was added to the titration vessel in small increments. Accurate concentrations of the NaOH solutions were determined by titration with a NORMEX

Table 1 RSV Active and Passive Loading in Liposome Formulations 10 mM Total Lipids (0.25 mM TPP3)

Lipid Composition	Loading Technique	EE%	[TPP3] (mM)	RSV/Lipids (Mole Ratio)	Δ2R (nm)	ΔPDI
DPPC/Chol (2:1)	Active	71	–	1:11	10 ± 4	0.23 ± 0.05
DPPC/TPP3/Chol (1.925:0.075:1)	Active	72	0.075	1:11	−16 ± 3	− 0.09 ± 0.04
DPPC	Passive	89	–	1:9	−3 ± 3	0.2 ± 0.02
DPPC/TPP3 (1.95:0.05)	Passive	69	0.23	1:12	−5 ± 3	~0
DOPC	Passive	93	–	1:9	−22 ± 3	~0
DOPC/TPP3 (1.95:0.05)	Passive	62	0.20	1:13	1 ± 2	0.08 ± 0.02

Notes: RSV/total lipids molar ratio for passive and active loading is 1:8. Δ2R and ΔPDI represent the variation of hydrodynamic size and PDI, with respect to the ones of the corresponding liposome formulation in the absence of RSV. Error associated with the determination of EE% is 5%.

Hydrochloric acid 0.1 mol/L (0.1 N) RPE standard solution (Supelco). The first part of the titration plot (up to 0.6 molar equivalents) was fitted using HYPERQUAD 2000.[48]

RSV Active Loading by pH Gradient Method

Generation and Determination of Transmembrane pH Gradient in Liposomes

Empty liposome formulations (15 mM total lipids) were prepared in 170 mM calcium acetate at pH 6, as described in the paragraph "Preparation of liposomes." The transmembrane pH gradient was generated by a dry filtration protocol; the acetate salt was removed from the bulk by gel-exclusion chromatography on Sephadex G50 mini-columns, pre-equilibrated with 150 mM PBS (pH = 7.4).[49] About 400 µL of the liposome dispersion was loaded onto a 5 mL mini-column and centrifuged at 1000 g for 10 min. About 450 µL of PBS was added to the top of the column, and another centrifugation cycle of 10 min was performed. Eluates from the two centrifugation cycles containing liposomes with pH gradient were collected.

The pH of the internal aqueous compartment of liposomes was measured using the water-soluble and pH-sensitive fluorescent probe pyranine, which was enclosed in the internal aqueous core, as described below. Pyranine-loaded liposomes (15 mM total lipids) were prepared as described in "Preparation of liposomes", hydrating the film with 0.5 mM pyranine in 170 mM calcium acetate (adjusted at pH = 6 by HCl 0.1 M). Filtration on Sephadex G-50 minicolumns (equilibrated in PBS) was used to generate the transmembrane pH gradient and to remove unentrapped pyranine. After filtration, the liposome suspension was diluted with PBS to a final lipid concentration of 4 µM, and p-xylene-bis-pyridinium bromide (DPX) was added (2 mM final concentration) to quench the fluorescence of any residual unentrapped pyranine. The fluorescence emission intensity of pyranine was measured at 507 nm by exciting the sample at 460 and 415 nm. The fluorescence emission spectra were recorded in a quartz cuvette of 1.0 cm path length on a Fluoromax-4 Horiba-Jobin Yvon spectrofluorimeter.

The ratio of fluorescence intensities, $R = I_{F460}/I_{F415}$ is related to internal pH, as described by Barenholz and Clerc[50]

$$2pH = pk_a + \log\frac{R - R_a}{R_b - R} \tag{2}$$

where pK_a is the apparent pK_a value of the fluorescent probe ($pK_a = 7.268 \pm 0.003$) and R_a and R_b refer to the ratios of the fluorescence intensities of the protonated and unprotonated forms of the probe, respectively ($R_a = 0.0122 \pm 0.0007$; $R_b = 2.515 \pm 0.006$). The internal pH value was monitored for three days after the establishment of the transmembrane gradient.

Loading of RSV

An appropriate volume of RSV solution in absolute ethanol was added to empty liposomes with a transmembrane pH

gradient (internal pH 8.2, external pH 7.4) to obtain a final 1:8 RSV/lipid molar ratio. In a typical loading experiment, 25 μL of 0.1 M RSV solution was added to 2 mL of empty liposomes dispersion (10 mM in total lipid). Liposomes were incubated in the presence of RSV for 1 h at 45°C, a temperature above the T_M, to increase the permeability of the lipid membrane and promote RSV inclusion. The volume of ethanol added to the aqueous dispersion of liposomes was kept below 2% of the total volume to have a negligible effect on the liposome structure.

Unentrapped RSV was removed by dialysis against PBS (membrane: 254.3 mm^2, cut-off: 14 kDa). Dialysis conditions (500 μL RSV-liposomes, 25-fold PBS volume, 30 min changes over 2.5 h) were fixed in preliminary experiments using RSV as the retentate solution (1.25 mM in PBS/absolute ethanol). The samples were protected from light during the process.

RSV Passive Loading

An appropriate volume of RSV solution in absolute ethanol (0.1 M) was added to the lipid mixture before film formation to obtain a 1:8 RSV/lipid ratio. In a typical experiment, 25 μL of 0.1 M RSV solution was added to the lipid mixture to obtain, after hydration, 2 mL of liposomes dispersion, 10 mM in lipids and 1.25 mM in RSV. Before freeze-thaw cycles, sonication at 40 W was carried out (10 cycles of 10 s, Sonics Vibra Cell sonicator) to break the RSV aggregates that usually form in aqueous solutions and improve RSV inclusion in the lipid bilayer.[51] Unentrapped RSV was removed by dialysis, as described in paragraph "RSV active loading using the pH gradient method". Empty liposomes were used for the comparison.

RSV Encapsulation Efficiency and in-vitro Release

The concentration of RSV loaded into the liposomes was evaluated by HPLC using a Waters Alliance 2695 instrument (Waters Associates, Milford, MA, USA) coupled with a photodiode array detector (PDA Waters 996). Data were collected and analyzed using Empower 2 software (Waters, Milford, MA, USA). Trans-stilbene (TSB) was used as internal standard (concentration 1×10^{-4} M). In the case of RSV-liposomes prepared by the passive loading technique, to break liposomal aggregates, samples were diluted (1:2) prior to injection with a methanol solution containing TSB at a concentration properly set to obtain a final concentration of TSB of 1×10^{-4} M. After the addition of MeOH, RSV-liposomes prepared by the active loading technique were further diluted (1:1) with MilliQ water before injection (injection volume 15 μL). The employed HPLC column was a C18-SunFire 150 × 4.6 mm ID, 3.5 μm (dp), and the mobile phases were water/acetonitrile 95/5 + 0.1% TFA (solvent A) and methanol + 0.1% TFA (solvent B). The elution gradient started with (A/B (80/20, v/v) in 7 minutes reached 100% B and maintains 100% B for 20 min. All solvents were filtered through 0.45 μm filters before use. The analysis was performed at 30°C with a flow rate of 1 mL/min. Each sample was injected in triplicate, and the average area was used to determine RSV concentration.

The entrapment efficiency (EE %) was then calculated using the following equation:

$$E.E.(\%) = \frac{[RSV]_{pd}}{[RSV]_o} 100 \tag{3}$$

where $[RSV]_{pd}$ indicates the RSV concentration after dialysis and $[RSV]_0$ indicates the concentration immediately after extrusion or at the beginning of the incubation process (in the case of active loading), as indicated in the corresponding paragraphs describing the loading protocols.

In-vitro RSV release from liposomes was evaluated using the dialysis method. RSV-loaded liposomes (3 mL) were placed in a 15 mL dialysis chamber with a dialysis membrane (cut-off of 14 kDa) of area 176.6 mm^2. The membrane was then placed in contact with 50-fold volume of 150 mM PBS. The system was maintained at 37°C and the diffusate solution was kept under gentle stirring for 48 h. About 0.25 mL of the liposome dispersion was withdrawn at regular intervals and the proper amount of diffusate dialysis buffer was discarded to maintain a constant ratio between the retentate and diffusate solutions. Samples were immediately analyzed by HPLC to assess RSV content.

Table 2 Trolox Active Loading in Liposome Formulations 10 mM in Total Lipids (0.25 mM TPP3)

Lipid Composition	Loading Technique	Incubation Time (h)	EE %	Trolox/Lipids (Mole Ratio)	Δ2R (nm)	ΔPDI
DPPC/Chol (2:1)	pH	1.5	78	15:1	50 ± 5	0.34 ± 0.08
DPPC/TPP3/Chol (1.925:0.075:1)	pH	1.5	66	13:1	85 ± 9	0.38 ± 0.09

Notes: Incubation is carried out at 20:1 Trolox/total lipids molar ratio. Δ2R (nm) and ΔPDI represent the variation of hydrodynamic size and PDI with respect to the corresponding liposome formulation, in the absence of Trolox. Error associated with the determination of EE% is 5%.

Loading of Trolox in Liposomes

Lipid composition of liposomal formulations used for loading Trolox is indicated in Table 2. Empty liposomes featuring a transmembrane pH gradient were prepared in 150 mM calcium acetate.

Trolox Stability in Calcium Acetate

Trolox stability in the internal aqueous cavity of liposomes was evaluated by registering upon time (24 h) UV absorption spectra of a 200 μM solution of Trolox in calcium acetate 150 mM at pH 8.2. Absorption spectra were recorded in the range 240–330 nm, in a 1.0 cm path length quartz cuvette on a Cary 300 UV–Vis double-beam spectrophotometer. Except for the measurements, all the samples were stored in the dark.

Trolox Active Loading by pH Gradient Method

To an appropriate volume of empty liposomes dispersion (0.25 mM in total lipid) featuring a transmembrane pH gradient (internal pH = 8.2, external pH 7.4), a proper amount of Trolox powder was added to obtain a 5 mM final Trolox concentration and 20:1 Trolox/lipid molar ratio. In a typical experiment, to 12.5 mg of Trolox, (9.99×10^{-3} mmol) 2 mL of liposomes dispersion (0.25 mM in total lipid) featuring a transmembrane pH gradient were added. After 1 h of incubation at 45°C, the unentrapped Trolox was removed by dialysis against a 25-fold external PBS volume, changing the external medium every 30 min for 2 h and maintaining the diffusate solution under stirring. These conditions were established through preliminary experiments using a 5 mM Trolox solution as the retentate. Both the incubation and dialysis were performed in the dark.

For comparison, Trolox loading based on a concentration gradient was considered. Empty liposomes (DPPC/Chol and DPPC/Chol/TPP3) without a transmembrane pH gradient were prepared in PBS 150 mM as described in "Liposome preparation". In a typical experiment, 2 mL of liposomes dispersion (0.25 mM in total lipid) were added to 12.5 mg of Trolox (9.99×10^{-3} mmol). The mixture was incubated for 1 h at 45°C, and unentrapped Trolox was removed by dialysis, as described above.

Trolox Encapsulation Efficiency and in-vitro Release

The encapsulation efficiency of Trolox in liposomes was evaluated by UV–Vis spectroscopy using a Cary 300 double-beam spectrophotometer. Before the measurements, the Trolox-loaded liposomes were disrupted by the addition of 2-propanol in a 1:1 volume ratio. Trolox concentration was then assessed using the absorbance maximum (290 nm) of the resulting solution. The EE % was calculated as for RSV (Eq. 3).

In-vitro Trolox release from liposomes was evaluated using the dialysis method. Trolox-loaded liposomes (10 mL) were placed in a 50 mL dialysis chamber with a dialysis membrane (cut-off of 14 kDa) of 615.4 mm^2. The membrane was then placed in contact with 50-fold volume of 150 mM PBS. The system was maintained at 37°C and the diffusate solution was kept under gentle stirring for the whole duration of the experiment. About 0.5 mL of liposome dispersion was withdrawn at regular intervals and the proper volume of diffuse dialysis buffer was discarded to maintain a constant ratio between the retentate and diffusate solutions. After collection, each sample was diluted 1:1 with 2-propanol to break liposomal aggregates and then analyzed to assess Trolox content by UV–Vis measurements, as described in the paragraph "Trolox stability in calcium acetate."

Evaluation of TPP3 Concentration in Liposome Dispersions

The concentration of TPP3 in dialyzed RSV-liposomes prepared by passive loading was evaluated by HPLC measurements following the same HPLC protocol used for the determination of RSV concentration (described in the paragraph "RSV Encapsulation Efficiency and in vitro release").

For liposomes prepared by the active loading technique, TPP3 concentration was evaluated by ^{1}HNMR, adopting the following protocol: 1) 2 mL of 10 mM dialyzed liposomes were dried using a rotary evaporator and then under high vacuum (0.4 mbar) for at least 6–8 h; 2) the residue was taken up with chloroform, transferred (including the precipitate) to a centrifuge tube, and centrifuged at 1000 × g for 10 min. The supernatant was placed in an NMR tube, and the organic solvent was gently removed under nitrogen flux; 3) 600 μL deuterated methanol, containing 3 mM dimethoxy(dimethyl) silane as an internal standard, was added to the dried sample. The following NMR signals were chosen to assess liposome composition: 5.26 ppm (m, 1 H, DPPC), 5.37 ppm (d, 1H, Chol), 7.80 ppm (m, 30H, TPP3), 0.11 ppm (s, 6 H, DDSi).

Biological Evaluation on Cell Cultures

Cell Lines

The immortalized murine skeletal muscle cell line C2C12 was seeded in a 96 multi-well dish at 400 cells/cm^2, cultured until confluence in 100 Dulbecco's Modified Eagle's medium (DMEM) supplemented with 1% L-glutamine, 2% HEPES, 0.5% gentamicin, and 20% FBS.

The human breast adenocarcinoma cancer cell line MDA-MB231 was cultured in high glucose Dulbecco's Modified Eagle's medium (DMEM) supplemented with 100 IU/mL penicillin, 100 IU/mL streptomycin, 1% L-glutamine, 1% non-essential amino acids, and Fetal Bovine Serum (FBS). Cell cultures were incubated in a humidified atmosphere (95% air/ 5% CO_2) at 37°C.

Cytotoxicity Evaluation

The MTT assay was used to determine the cytotoxicity of the liposome formulations in C2C12 and MDA-MB231 cells. This test is based on the quantification of a tetrazolium salt (3-[4,5-dimethylthiazol-2-yl]-2,5 diphenyl tetrazolium bromide), which is converted into formazan salt by mitochondrial dehydrogenases, thus providing an indirect measure of both cell viability and mitochondrial metabolic functionality. Cells were treated with liposome formulations at different concentrations (0.005–0.04 mM for C2C12 and 0.005–0.1 mM for MDA-MB231) and incubated for 24, 48 and 72 hours, then 10 µL of MTT solution (5 mg/mL in PBS) was added and incubated for 3 hours at 37°C. Finally, the medium was removed and 200 µL of DMSO was added to each well and incubated for 20 min at 37°C. Cell viability was determined by quantifying cell metabolic activity.[52] Absorbance was measured at 570 nm using a plate reader.

The results are expressed as mean ± SD and are representative of three independent experiments performed in triplicate. Statistical significance was assessed using Student's *t*-test, calculated with Microsoft Excel, with significance thresholds set at $p < 0.05$, $p < 0.005$, and $p < 0.001$.

Mitochondrial Co-Localization by Confocal Microscopy

Laser scanning confocal microscopy (LSCM) was used to study the intracellular distribution of liposomes. Cells grown for 24 h on 12 mm glass coverslips were incubated for 4 and 18 h with 0.025 mM and 0.1 mM fluorescent liposome formulations, tagged with Rhod-PE. At the end of the treatment, cells were incubated with MitoTracker probe (400 nM) for 15 min and then fixed with 1% paraformaldehyde in PBS for 10 min at room temperature. Observations were performed using a Leica TCS 4D confocal laser scanning microscope (Leica Microsystems, Mannheim, Germany) equipped with an Ar/Kr laser. After excitation of MitoTracker (at 488 nm) or Rhod-PE included in liposomes (at 568 nm), fluorescence signals were collected using a 590 nm band-pass filter.

Semi-quantitative analysis of mitochondrial colocalization was performed by calculating Manders' coefficient (M) using ImageJ, following the procedure described by Dunn et al.[53]

Flow Cytometry Analysis of Mitochondrial Membrane Potential

The analysis of mitochondrial membrane potential was performed by using the cationic fluorescent probe tetramethyl-Rhodamine methyl ester (TMRM, Thermo Fisher Scientific, Waltham, MA). MDA-MB231 cells were seeded in MW6

(1.5×10^5 cells/well); after 24 hours they were treated with different concentrations of DPPC, DPPC/TPP3, DPPC/Chol/TPP3, DOPC/TPP3 liposomal formulations (0.005–0.01-0.02–0.04-0.1 mM).

At the end of treatment, cells were detached with EDTA and trypsin, resuspended in PBS and labelled with TMRM (5 µg/mL, 15 min at 37°C). Samples were then immediately analyzed with a FACSCalibur flow cytometer (Becton, Dickinson and Company, Franklin Lakes, New Jersey, USA). Fluorescence emission (FL2) was collected through a 575 nm band-pass filter to analyze TMRM signal. At least 10,000 cells per sample were acquired in log mode. Median values of FL2 channel were calculated through the CellQuest software (Becton, Dickinson and Company). The results are expressed as mean ± SD from two independent experiments. Statistical analysis was performed using Student's *t*-test by Microsoft Excel (significance thresholds set at $p < 0.05$; $p < 0.005$; $p < 0.001$).

Results and Discussion

Characterization of TPP3-Liposomes: Effect of TPP3 Bolaamphiphile and Cholesterol on Saturated and Unsaturated PC Liposomes

DPPC- or DOPC-based liposomes containing different amounts of TPP3 were investigated to understand the effect of TPP3 on vesicles. The influence of the preparation protocol was also studied by comparing the same formulation prepared by simple extrusion or extrusion preceded by sonication, which is a step required in the passive loading protocol to increase RSV entrapment. The hydrodynamic diameter and polydispersity (PDI) of the mixed vesicles determined using DLS are shown in Figure 3.

The presence of TPP3 affects the organization of the phospholipid bilayer membrane and the formation of liposomes as a function of the nature of the PC hydrophobic chains, while the sonication step seems to be irrelevant to liposome size and polydispersity for both DOPC- and DPPC-based liposomes, as no difference was observed with respect to the non-sonicated liposomes (data not shown). The diameter and PDI of DOPC-based aggregates were characteristic of liposomal vesicles, with size around 100 nm, as expected using a 100-nm extrusion filter, in all the explored TPP3 concentration range (0–20%). On the contrary, for DPPC-based liposomes above 10% TPP3, DLS correlation functions deviated from a single exponential decay, providing evidence of a more complex behavior. The observed behavior of TPP3 in a mixture with saturated or unsaturated phospholipids is in line with experimental evidence previously reported in the literature for vesicle including bolaamphiphiles. In these studies, the maximum percentage of bolas in the formulation varied depending on both the chemical nature of the

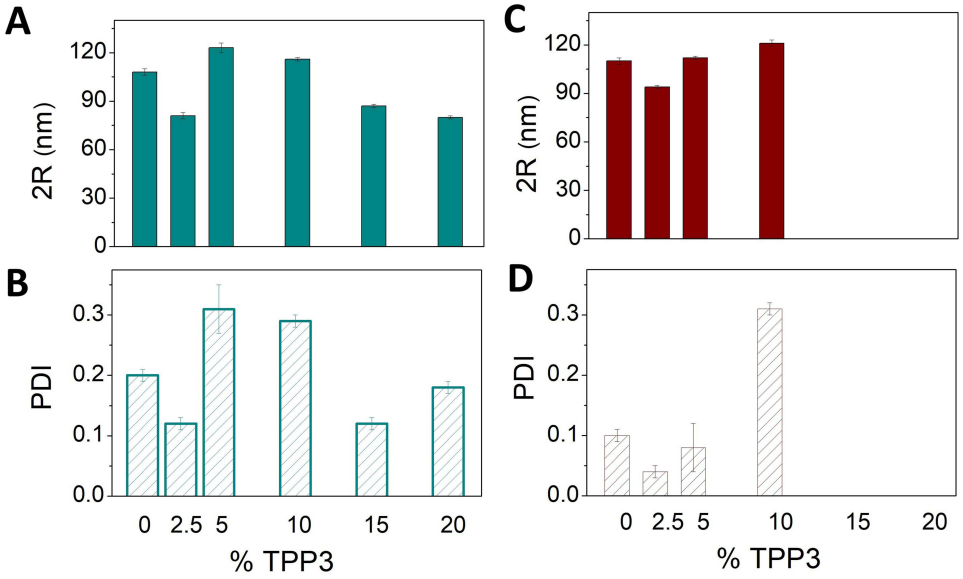

Figure 3 Hydrodynamic size 2R and PDI for DOPC (**A** and **B**) or DPPC (**C** and **D**) based liposomes with increasing amount of TPP3. In the case of DPPC, liposome formation is not observed beyond 10% TPP3. Errors are the SD calculated on three series of measurements on at least three different samples.

https://doi.org/10.2147/IJN.S539303

bolaamphiphile and the molecular structure of the PC.[54,55] For example, a bolaamphiphile with a bulky aromatic head, similar to TPP3, can form stable vesicles with the saturated phospholipid DPPC only up to 3.2%[54] whereas an anionic C30 bolaamphiphile can form stable vesicles with the partially unsaturated egg-PC up to 10%.[55]

The absolute scattering intensity and vesicle size vs temperature were investigated by DLS to evaluate the lipid melting transition temperature (T_M) as a function of TPP3 amount in the lipid bilayer membrane. This investigation also provides information on the preferential conformation (hairpin or extended) that TPP3 adopts inside the liposome membrane. In Figure 4, the plot of the absolute scattering intensity shows that the T_M value does not change with increasing TPP3 amount. However at the highest TPP3, the jump at T_M spans over a wider range of approximately 10°C. This indicates the low cooperativity of the transition, associated with lower DPPC-TPP3 miscibility,[56] suggesting a relationship between the formation of TPP3 domains and bilayer membrane stabilization. It also suggests that TPP3 could adopt a predominantly extended conformation within the lipid bilayer membrane, which is more favorable for long-chain molecules, and excludes a hairpin arrangement as well as its subsequent detergent effect, which is usually accompanied by a decrease in T_M.[54] Assuming the extended conformation for TPP3, the formation of domains is also favored by the hydrophobic mismatch due to the different length of the hydrophobic portion of the phospholipid and the bola, as it has already been reported for other bolas with C20 chains.[57]

Cholesterol was added to the liposomes to obtain a lipid bilayer membrane with optimal features for RSV and Trolox entrapment in the preparation by the active gradient method. Indeed, drug loading using the gradient method typically involves the use of liposomes with membranes composed of cholesterol and lipids with high transition temperatures. Thus, they are very dense and compact, such that the pH gradient is maintained and trapped solutes are retained.[58] Based on literature and data previously collected by some of us which evidenced low gradient stability for DOPC-based formulations,[59] we considered only DPPC-based liposomes, where Chol was added at a fixed amount to maintain a constant molar ratio with respect to the sum of DPPC and TPP3, whereas the total concentration of the components was fixed at 15 mM. The effect of increasing TPP3 content (up to 10%) on liposome size was studied.

The internal pH of liposomes containing TPP3 up to 5% was monitored for 72 h by fluorescence spectroscopy, as described in the Materials and Methods section. Soon after preparation, the internal pH was 8.2 and it remains stable at approximately 8.0 ± 0.2 for the subsequent 72 h for all formulations.

Liposome dispersions formulated with TPP3 up to 5% feature a monomodal distribution of vesicles (Figure 5), with diameters consistent with the extrusion membrane. When TPP3 was added at 10% to the formulation, both the average size and the PDI increased. Size distribution analysis indicated that two populations of aggregates were formed, one with a diameter of approximately 130 nm and the other with a larger size (approximately 600 nm). Any attempt to purify this dispersion by filtration on PTFE filters of 450 nm was ineffective, suggesting that the largest aggregates were in equilibrium with the smallest ones.

Stability of liposomal formulations has been evaluated on liposomal formulation with the lowest TPP3 content (2.5%). The size of all the formulations was stable over a period of 14 days (see Supplementary Material Figure S1). As expected, the presence of TPP imparts a positive charge to liposome, as evidenced by the positive values of ζ-potential (see Supplementary Material Figure S2). After one week, in DPPC/Chol/TPP3 and DOPC/TPP3 liposomes the ζ-potential switches to negative values, which is indicative of a reorganization of TPP3 molecules in liposomes with a fluid bilayer membrane (see Supplementary Material Figure S2). To evaluate the behavior of the formulations in the biological media used for cell cultures, stability of the samples has been studied also in the presence of Fetal Bovine Serum (FBS), which has been added in a volume ratio of 20% to 1 mM liposomes. Negative values of ζ-potential in all formulations indicate that serum proteins always adsorb on liposomes, independently on lipid composition and surface charge. Time stability in FBS is strictly dependent on liposome composition (see Supplementary Material Figure S2). It is interesting to note that the presence of TPP3 is able to counteract or limit the tendency of liposomes to aggregate, which is more rapid and marked for DPPC/Chol and DOPC-liposomes.

All these findings indicate that: (i) the influence of TPP3 on the organization of phospholipid bilayer membrane depends on the nature of the PC hydrophobic chains as well as on the presence of cholesterol, in particular higher percentage of TPP3 in DPPC liposomes results in non-monomodal distribution of size, both in presence and absence of Cholesterol; (ii) TPP3 seems to adopt in the bilayer membrane an extended conformation and very likely is organized in domains; (iii) DPPC/Chol TPP3-liposomes with TPP3 up to 5% proved to be stable in dimensions and internal pH, resulting suitable for the loading of RSV and Trolox by the active gradient method.

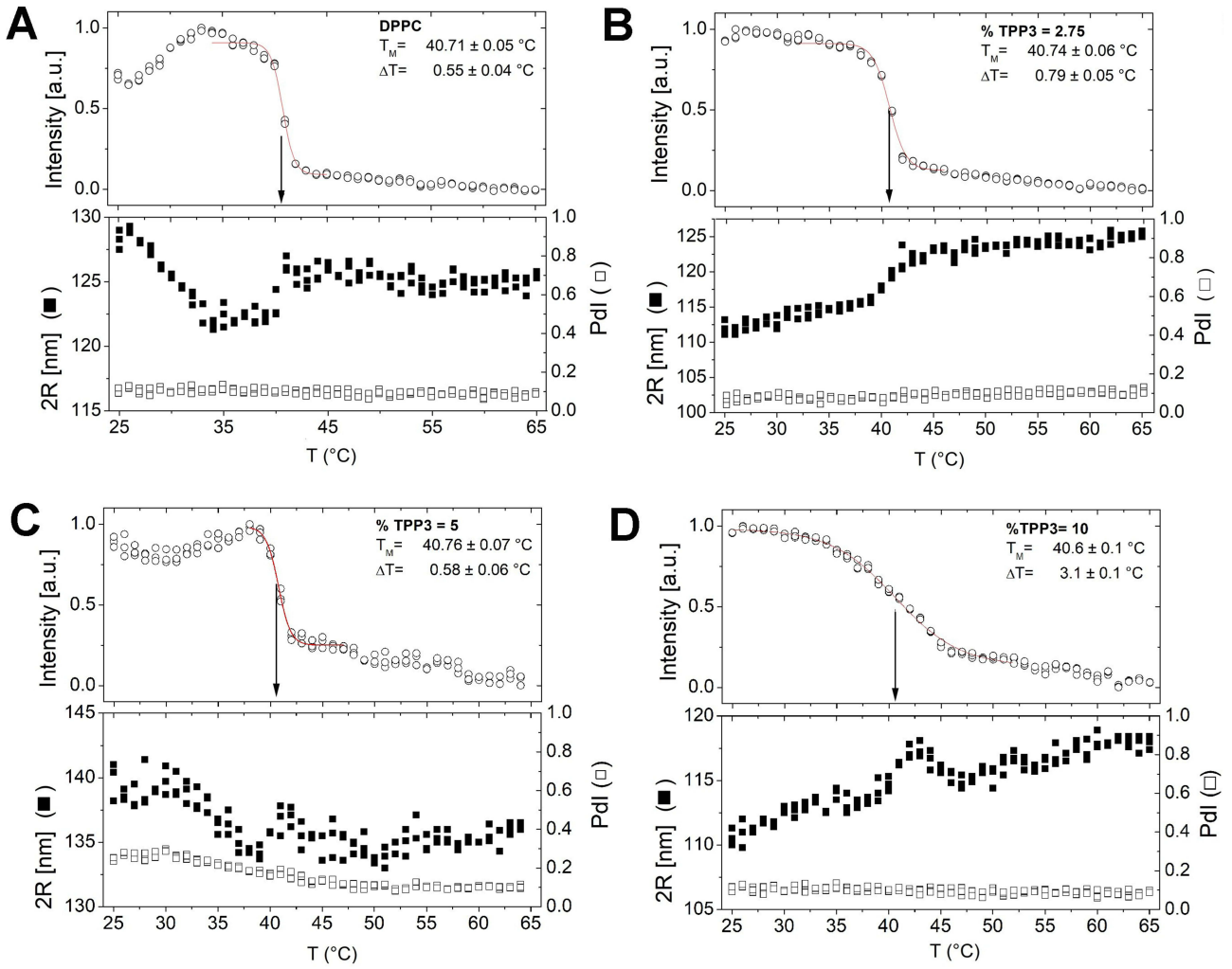

Figure 4 Normalized intensity as a function of temperature for DPPC (**A**); DPPC/TPP3 97.5:2.5 (**B**); DPPC/TPP3 95:5 (**C**); DPPC/TPP3 95:10 (**D**). T_M is determined by a Boltzmann sigmoidal fit (red line) and is marked by a vertical arrow. For each temperature, the three different measurements of the intensity data have been reported and used for curve fitting.

Biological Evaluation of TPP3-PC and TPP3-PC/Chol Liposomes

Cytotoxicity by MTT Assay

The biocompatibility of empty TPP3-liposomes was evaluated by MTT assay on both the murine skeletal muscle cell line C2C12 and the human breast cancer cell line MDA-MB231, because toxicity depends not only on the specific liposome formulation but also on the characteristics of the cell type. Liposomal formulations with TPP3 below 5% in moles relative to total lipid were used for toxicity assessment, based on data reported in the literature indicating that TPP derivatives are typically used in concentrations between 1 and 8%.[8–12]

C2C12 cells were treated with liposomes formulated with 2.5 and 5% of TPP3 at various total lipid concentrations. It was immediately evident that only liposomes formulated with 2.5% of TPP3 show acceptable toxicity while toxicity becomes too high at 5% TPP3 percentage (data not shown). The DPPC/TPP3 and DOPC/TPP3 liposomes showed the same dose-dependent reduction in cell viability. In Figure 6A, we report as an example the analysis of cell viability at 24, 48, and 72 h after the treatment with DPPC-liposomes formulated with 2.5% of TPP3. DPPC/Chol based liposomes were less toxic and better tolerated than DPPC based liposomes at all the tested concentrations (Figure 6B).

The MTT assay was also performed on MDA-MB231 cells (Figure 7). The analysis of cell viability was analyzed after the treatment with DPPC/TPP3, DOPC/TPP3, DPPC/Chol/TPP3 (TPP3 2.5%) liposomes for 24, 48, and 72 h. All formulations induced a dose-dependent decrease in cell viability, the DPPC/Chol liposomes being less toxic and well

https://doi.org/10.2147/IJN.S539303

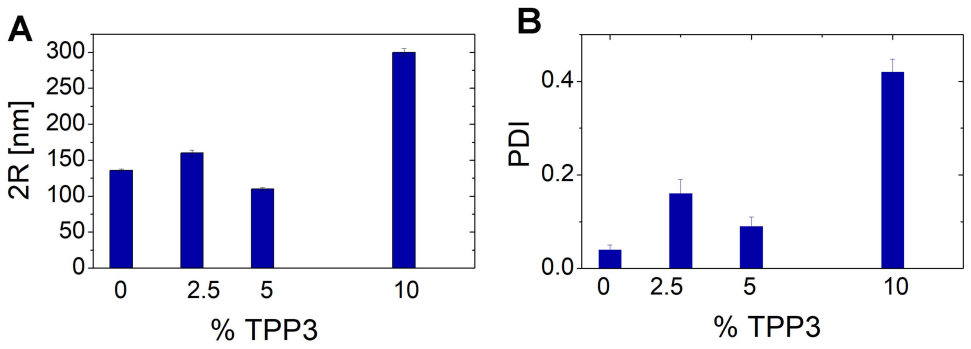

Figure 5 Hydrodynamic diameter 2R (**A**) and PDI (**B**) for DPPC-Chol-based liposomes, at increasing amount of TPP3. Results are expressed as mean ± SD values on three series of measurements on at least three different samples.

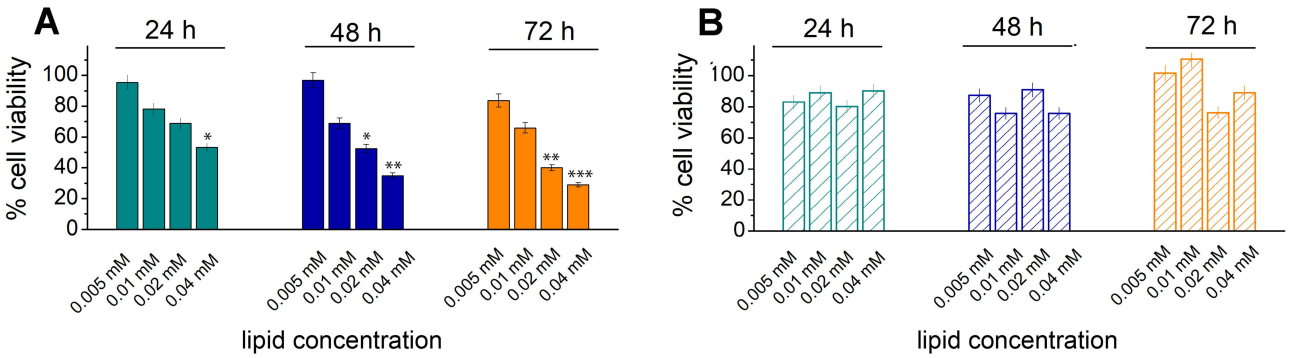

Figure 6 MTT assay performed on C2C12 cells to test cell viability over time. Cells were treated with increasing concentration of DPPC/TPP3 liposomes (**A**); DPPC/Chol/TPP3 liposomes (**B**). TPP3 is 2.5% with respect to all the lipid components. Data are expressed as % of cell viability with respect to control (set at 100% value). All experiments were conducted in triplicate in at least three independent experiments. Results are expressed as mean ± SD values. *p < 0.05; **p < 0.005; ***p < 0.001 vs control by Student's *t* test.

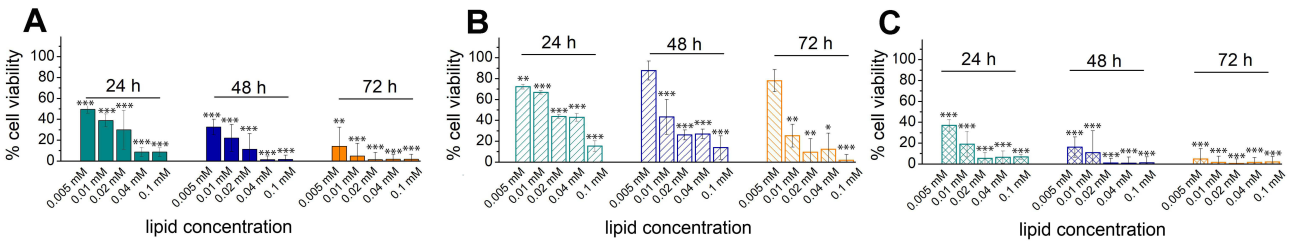

Figure 7 MTT assay performed on MDA-MB231 cells to test cell viability over time. Cells were treated with increasing concentration of: DPPC/TPP3 liposomes (**A**); DPPC/Chol/TPP3 liposomes (**B**); DOPC/TPP3 liposomes (**C**). TPP3 is 2.5% with respect to all the lipidic components. Data are expressed as % of cell viability with respect to control (set at 100% value). All experiments were conducted in triplicate in at least three independent experiments. Results are expressed as mean ± SD values. *p < 0.05; **p < 0.005; ***p < 0.001 vs control by Student's *t* test.

tolerated at the lowest concentration, similarly to what observed in C2C12 cells. Conversely, both the formulations without cholesterol were more toxic, with DOPC-based formulations being more toxic than DPPC-based formulations at all explored concentrations.

The results reported in this section and the IC_{50} values, summarized in Table 3, show that: (i) DOPC/TPP3 and DPPC/TPP3 (TPP3 2.5%) in the presence and in the absence of cholesterol, both show a good biocompatibility with skeletal muscle cells C2C12; (ii) tumor cells MDA-MB231 are more sensitive to the composition of liposome formulations, probably because of the strong dependence of tumor cells on energy metabolism and/or different interactions of

Table 3 IC_{50} (mM) of Different Liposome Formulation on C2C12 and MDA-MB231 Cells

Liposome Formulation	IC_{50} (mM)	
	C2C12	MDA-MB231
DPPC/TPP3	0.04	0.005
DPPC/Chol/TPP3	>0.04	0.017
DOPC/TPP3	–	<0.005

Notes: Values represent the concentration required to inhibit 50% of cellular activity; "–" indicates undetermined data.

vesicles with tumor cell membranes; (iii) for both cell lines DOPC-based liposomes resulted more toxic than DPPC-based ones; (iv) the presence of cholesterol in DPPC/Chol liposomes seems to protect both skeletal and tumor cells.

Mitochondrial Targeting

The ability of TPP3-liposomes to target mitochondria was explored in two cell lines, C2C12 and MDA-MB231. Mitochondrial co-localization was investigated for the formulations containing the 2.5% of TPP3 since biocompatibility studies showed that at higher ratios of the bolaamphiphile liposomes significantly altered the structure of mitochondria and had a marked toxic effect on both cell lines. After incubation with rhodamine-fluorescent liposomes, cells were labelled with MitoTracker, a probe widely used to reveal mitochondria.

LSCM images of C2C12 cells treated with TPP3-liposomes, shown in Figure 8, clearly indicate that TPP3-liposomes (red signal) interacted with the target mitochondria (green signal) and fused with them (yellow signal). Notably, the interaction with liposomes modifies the morphology of the mitochondria, whose structure appears less defined; however, as indicated by biocompatibility studies, cells are still viable.

LSCM images of MDA-MB231 cells treated with TPP3-liposomes are shown in Figures 9 and 10, with PC and PC-Chol liposomes used as a negative control (Figure 9A and C, respectively). DPPC-liposomes (TPP3 0%) scarcely entered human breast adenocarcinoma MDA-MB231 cells after 4 h of interaction with cultures (Figure 9A). The inclusion of TPP3 in the formulations noticeably increased their targeting capability, as shown in Figure 9B, where DPPC/TPP3-liposomes showed a marked ability to interact with tumor cells and appeared clusterized on the cell membrane (red signal) and co-localized with mitochondria into the cytoplasm (yellow signal). The presence of cholesterol in DPPC/Chol/TPP3-liposomes did not affect the interaction of liposomes with cells, although in this case, penetration into the cytoplasm and mitochondria was less effective (Figure 9D).

In addition, in the case of DOPC-based liposomes, TPP3 was crucial for targeting the mitochondria of MDA-MB231 cells (Figure 10A and B). DOPC/TPP3-liposomes entered cells more quickly than DPPC/TPP3-liposomes after 4 h of incubation with MDA-MB231 cells (Figure 10A). Indeed, no red signal was detected on the cell membrane, whereas a strong yellow signal came from the colocalization regions inside the cytoplasm (Figure 10A). The collapse of mitochondria and an evident reorganization of cytoplasmic structures were revealed when the incubation lasted 18 h (Figure 10C). These results could account for the large decrease in viability observed in cultures treated with the DOPC/TPP3-liposomes (Figure 7).

Effect of TPP3-Liposomes on Mitochondrial Function and Membrane Potential

The mitochondrial targeting ability shown by TPP3 liposomes could induce alterations of mitochondrial functionality. MTT results clearly indicated a dose-dependent cell viability reduction induced by all TPP3 formulations, mostly in MDA-MB231 cells. Then, we evaluated in this cell line the mitochondrial function through a membrane potential assay by using TMRM, a cationic red-fluorescent probe tetramethyl-Rhodamine methyl ester.[60] TMRM localizes in mitochondria where its fluorescent intensity directly correlates with mitochondrial membrane potential. Flow cytometry analysis revealed that a dose-dependent hyperpolarization effect could be detected even at 4 hours of cell incubation with liposomal formulations,

https://doi.org/10.2147/IJN.S539303

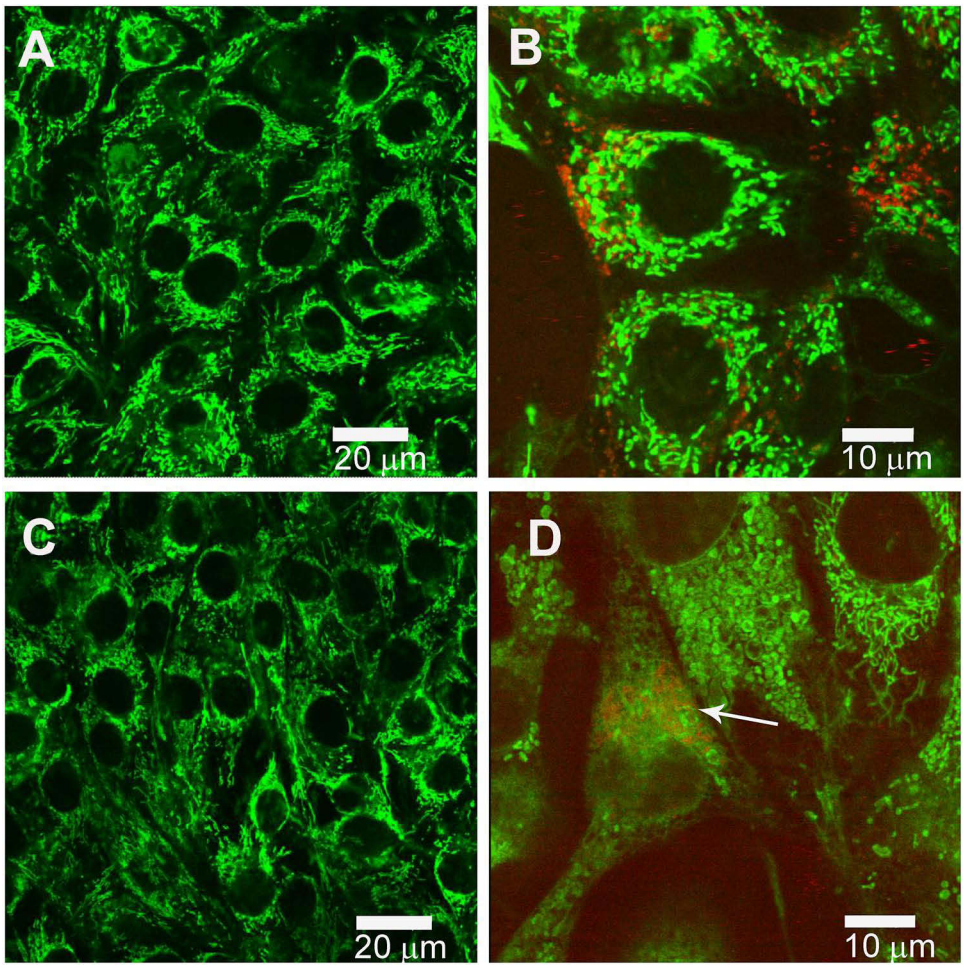

Figure 8 LSCM images of C2C12 cells labelled with MitoTracker probe (green signal), for 24 (**A** and **B**) and 48h (**C** and **D**), untreated (**A** and **C**) or treated with DOPC/TPP3-liposomes (red signal), (**B** and **D**). The arrow in (**D**) indicates the co-localization area.

as shown by the increase of fluorescent signal as compared to untreated samples (Figure 11 and Supplementary Material Figure S3). As expected, no alterations were observed in cells treated with DPPC liposomes (0% TPP3), confirming that this effect was closely dependent on TPP3 presence and on the concentration. As the cationic nature of TPP-bolaamphiphiles is strongly responsible for mitochondrial targeting,[10,11] we could hypothesize that the consequent mitochondrial membrane structure alterations due to new lipid incorporation could be correlated with a membrane hyperpolarization effect. Recently, it was demonstrated that a genetic model of increased mitochondrial membrane potential showed a phospholipid remodeling pattern which was able to induce nuclear DNA hypermethylation and regulation of mitochondrial, carbohydrate and lipid gene transcription.[61] Therefore, it can be hypothesized that in our model the employment of mitochondriotropic liposome formulations could affect lipid composition of mitochondrial membrane, thus inducing an increase of its potential. Moreover, a number of literature data correlate the mitochondrial membrane hyperpolarization with the increase of reactive oxygen species production and induction of cell death mechanisms.[62,63] Accordingly, the dose-dependent decrease of cell viability detected by MTT assay in TPP3 formulation-treated MDA-MB231 cells could be related to mitochondrial membrane structure alteration and its consequent hyperpolarization. In addition, the reduced toxic effect induced by the lower concentrations of TPP3 in DPPC/Chol/TPP3-liposomes (see the paragraph d "Cytotoxicity by MTT assay") is in agreement with their reduced effect on mitochondrial membrane as detected by TMRM labelling both at 4 and 24 hours. Conversely, DOPC-based formulations showed a stronger mitochondrial hyperpolarization effect than the other formulations even at 4 hours and with the lower concentrations (0.005, 0.01, 0.02 mM), probably explaining their higher toxicity observed in MDA-MB231 cells by MTT assays.

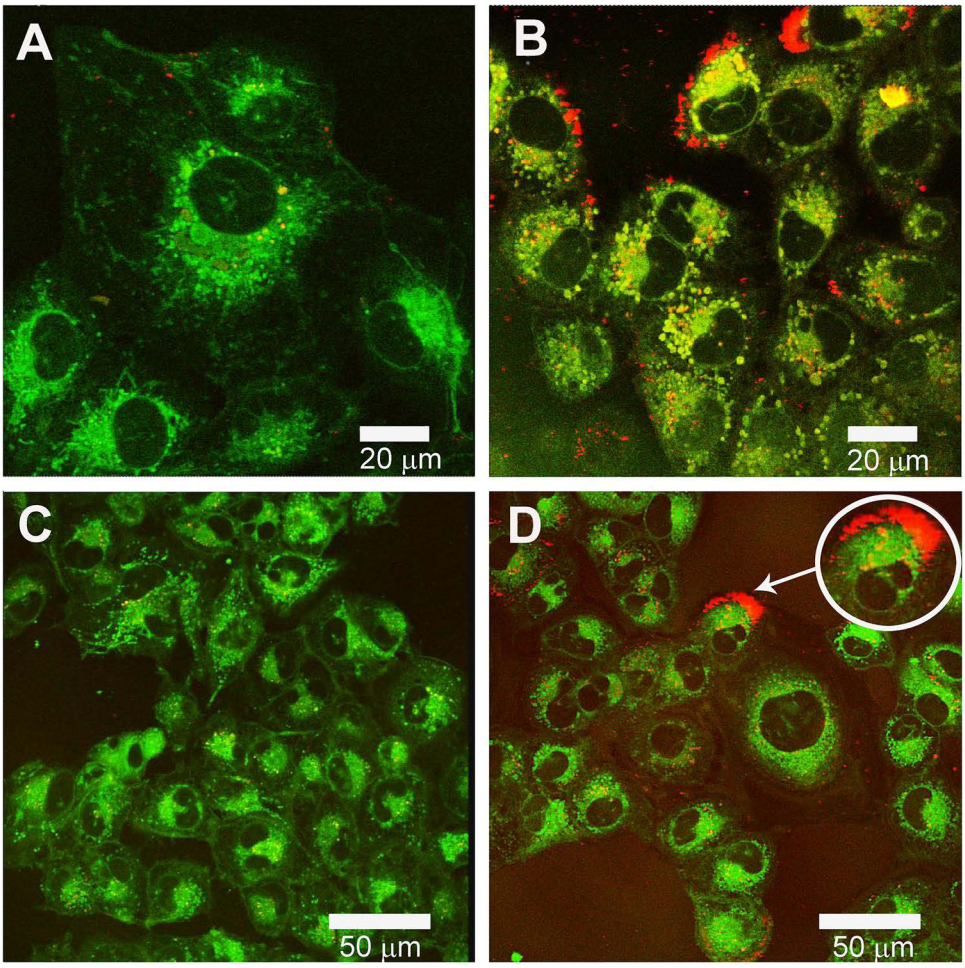

Figure 9 LSCM images of MDA-MB231 cells labelled with MitoTracker probe (green signal), treated with DPPC-based liposomes, in the absence (**A**) and in the presence (**B**) of TPP3 or DPPC/Chol-based-liposomes, in the absence (**C**) and in the presence (**D**) of TPP3. In the circular inset in (**D**), showing a magnification of the cell marked by the arrow, yellow spots indicating co-localization are visible.

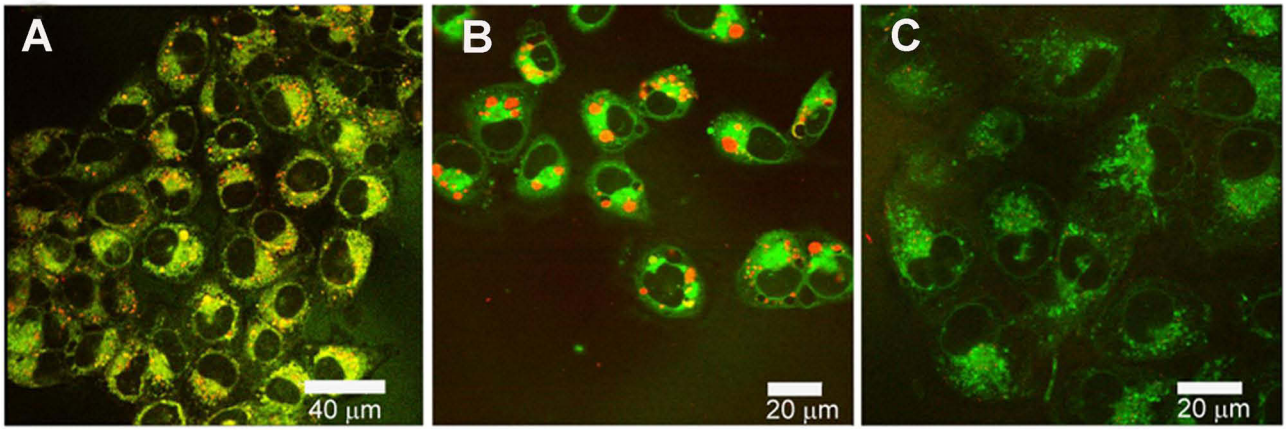

Figure 10 LSCM images of MDA-MB231 cells labelled with MitoTracker probe (green signal), treated with DOPC-based liposomes, in the presence (**A** and **B**) or in the absence (**C**) of TPP3, for 4 (**A** and **C**) and 18 h (**B**).

https://doi.org/10.2147/IJN.S539303

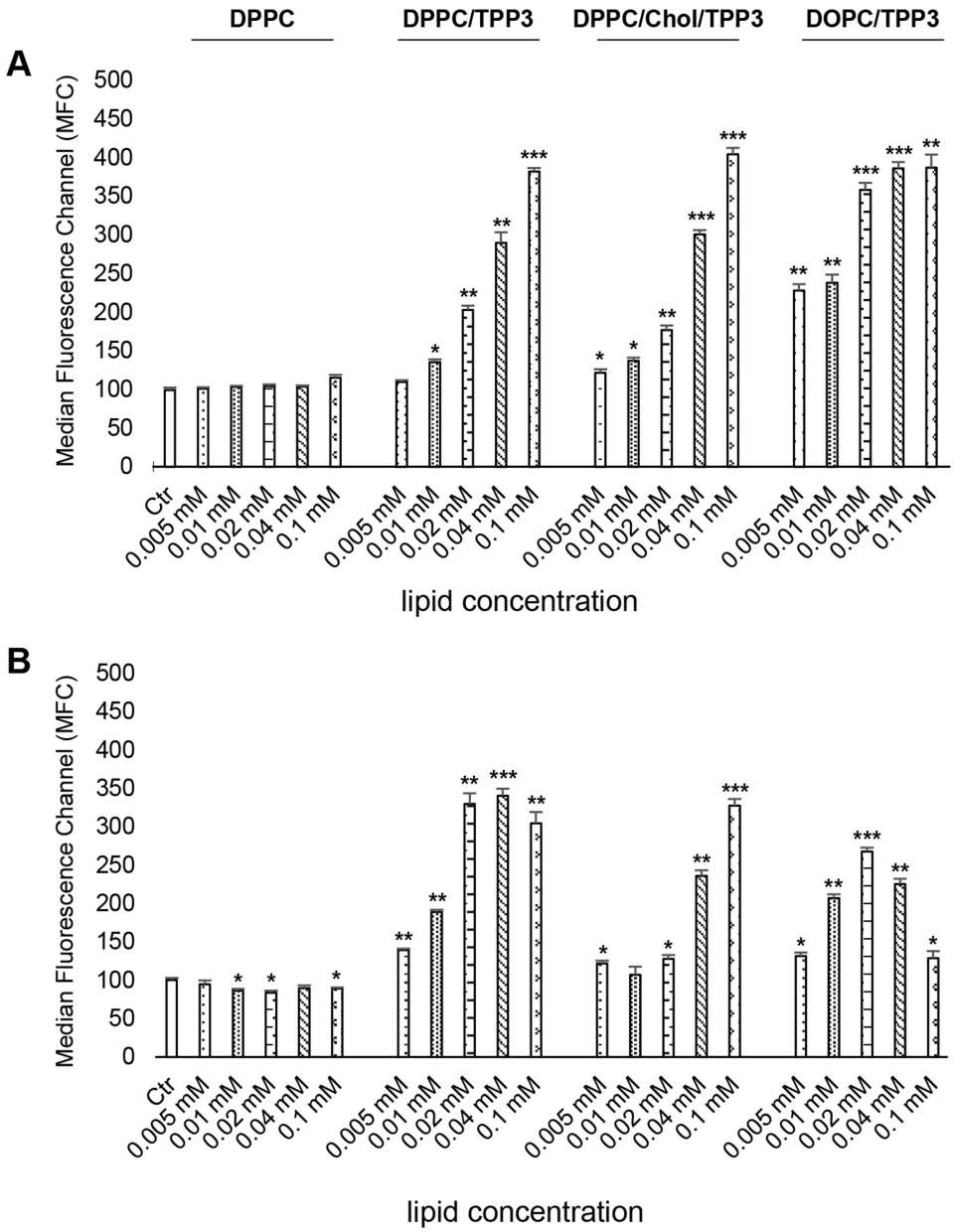

Figure 11 Flow cytometry analysis of mitochondrial membrane potential performed on MDA-MB231 cells labelled with the cationic fluorescent probe tetramethyl-Rhodamine methyl ester (TMRM). Cells were treated for 4 (**A**) and 24 hours (**B**) with increasing concentration of DPPC, DPPC/TPP3, DPPC/Chol/TPP3 and DOPC/TPP3 liposomes. Histograms show the median values of FL2 channel (MFC), corresponding to TMRM fluorescent signal, from control (Ctr) and treated samples. Results are expressed as mean ± SD values from two independent experiments. *p < 0.05; **p < 0.005; ***p < 0.001 vs Ctr (Student's *t*-test).

Summarizing, results from biological characterizations point out that the TPP3 bolaamphiphile allows obtaining mitochondriotropic liposomes even if present in small amounts in the formulation, as observed for other triphenylphosphonium derivatives, such as STPP or more complex lipid derivatives.[8,10,12] With regard to toxicity, comparison with other TPP derivatives reported in the literature is tricky, due from one side to the different experimental conditions used (cell types, toxicity test and assessment times) and from the other to the different lipid formulation that affects targeting efficiency and toxicity, as demonstrated by the results reported in this work. In any case, while the toxicity of DPPC/Chol/TPP3 liposomes on C2C12 is comparable to that of the less toxic derivatives reported in the literature,[8,10,12] the toxicity of all formulations detected in MDA-MB231 cells is higher and more similar to STPP-formulations. However, interestingly for TPP3-formulations, toxicity is triggered by a mechanism different from that of STPP; in fact, it is known

that STPP induces depolarization of the mitochondrial membrane,[8] while in our breast cell model TPP3-containing liposomal formulations induce hyperpolarization.

Loading of Antioxidants in Mitochondriotropic Liposomes

RSV-Loaded Liposomes

It has been demonstrated that inclusion in liposomes greatly enhances RSV solubility and reduces its degradation and isomerization to the less biologically effective cis form.[64,65] Moreover, several studies have reported better biological activity of liposomal RSV compared to free compounds.[66] In particular, as far as MDR reversal, liposomal RSV, combined with or co-delivered with anticancer drugs, has been shown to be effective against resistant tumors and to improve the efficacy of drugs in drug-sensitive tumors.[67,68] To the best of our knowledge, only a few studies have reported mitochondriotropic RSV-loaded liposomes[67,69,70] (only two concerning resistant tumors), whereas other RSV-loaded liposomes have been described as being cell- or tissue-specific.[71–74] For the preparation of mitochondriotropic RSV-loaded liposomes, we chose only 2.5% TPP3 formulations as they were non-toxic or had low toxicity, and explored two different methods: i) the active loading into the liposome aqueous core, exploiting the acidic properties of RSV phenolic functions, ii) the passive loading inside the lipid bilayer membrane, exploiting the low solubility of RSV in aqueous solution.

RSV Stability as a Function of pH and Determination of pK_a

To consider the active loading method, it is necessary to determine the acidity constant of RSV and assess RSV stability as a function of pH to select suitable conditions for obtaining stable RSV-loaded liposomes with a high encapsulation efficiency. A preliminary investigation was carried out to evaluate the transmembrane pH gradient of liposomes required to achieve RSV loading and to determine whether RSV was stable under such pH conditions.

As already reported in the literature for other buffer solutions,[75] RSV stability changes as a function of pH; in fact, under weakly acidic and neutral conditions (pH 5.5–7.5) the molecule is stable over time, and degradation is observed under basic conditions, being slight at pH 8 and more pronounced at pH 9 (Figure 12).

Although a large number of studies have reported the pK_a of RSV, these results are hampered by the low solubility (< 1 mg/mL) of RSV in water, which often affects the reliability of the results.[76] Because of this limitation, different techniques have been used to carry out these measurements, such as gel electrophoresis,[77] fluorescence spectroscopy[73] and UV–Vis spectrophotometry.[78]

In the present work, we report the measurement of the first acid dissociation constant of RSV (pK_{a1}) based on extrapolation of pK_{a1} by a series of potentiometric measurements in $EtOH/H_2O$ mixtures with decreasing ethanol concentration. Such an approach is sometimes used in the literature for the determination of pK_a whenever measurement in pure water is not feasible.[79] Given the high solubility of the compound in ethanol, homogeneous aqueous solutions can be prepared with this cosolvent at millimolar concentrations (2–5 mM). Titration was performed by adding a standard NaOH solution to the solvent mixture. In the experiments, the titrant was added up to 0.5–0.6 molar equivalents to avoid RSV decomposition due to the pronounced reactivity of the mono-anion in polymerization[75] and oxidation reactions.[79–81] A value of $pK_{a1} = 7.62 \pm 0.13$ for the first acid dissociation constant of RSV was obtained in pure water (see Supplementary Material, Figure S4).

RSV Active Loading Protocol

This protocol was developed only for DPPC/Chol based liposomes, which display a less permeable membrane and allow the pH gradient to be maintained for several days, as described in "Effect of Cholesterol on DPPC/TPP3 liposomes".

The protocol involved the addition of an ethanolic RSV solution to a solution of preformed liposomes with a pH gradient, followed by incubation. Initially, we explored different RSV/lipid mole ratios (1:8 and 1:20) and different incubation temperatures (30, 45, and 60°C) to set conditions that would result in a high RSV trapping efficiency while preventing its degradation. The optimal loading conditions required an RSV/lipid ratio of 1:8 and incubation at 45°C for 1 h, ie under conditions of good liposome membrane permeability. The inclusion of RSV in the liposomes led to a change in the size of the aggregates, as evaluated by DLS analysis (Table 1). The increase in the size of the DPPC/Chol

 https://doi.org/10.2147/IJN.S539303

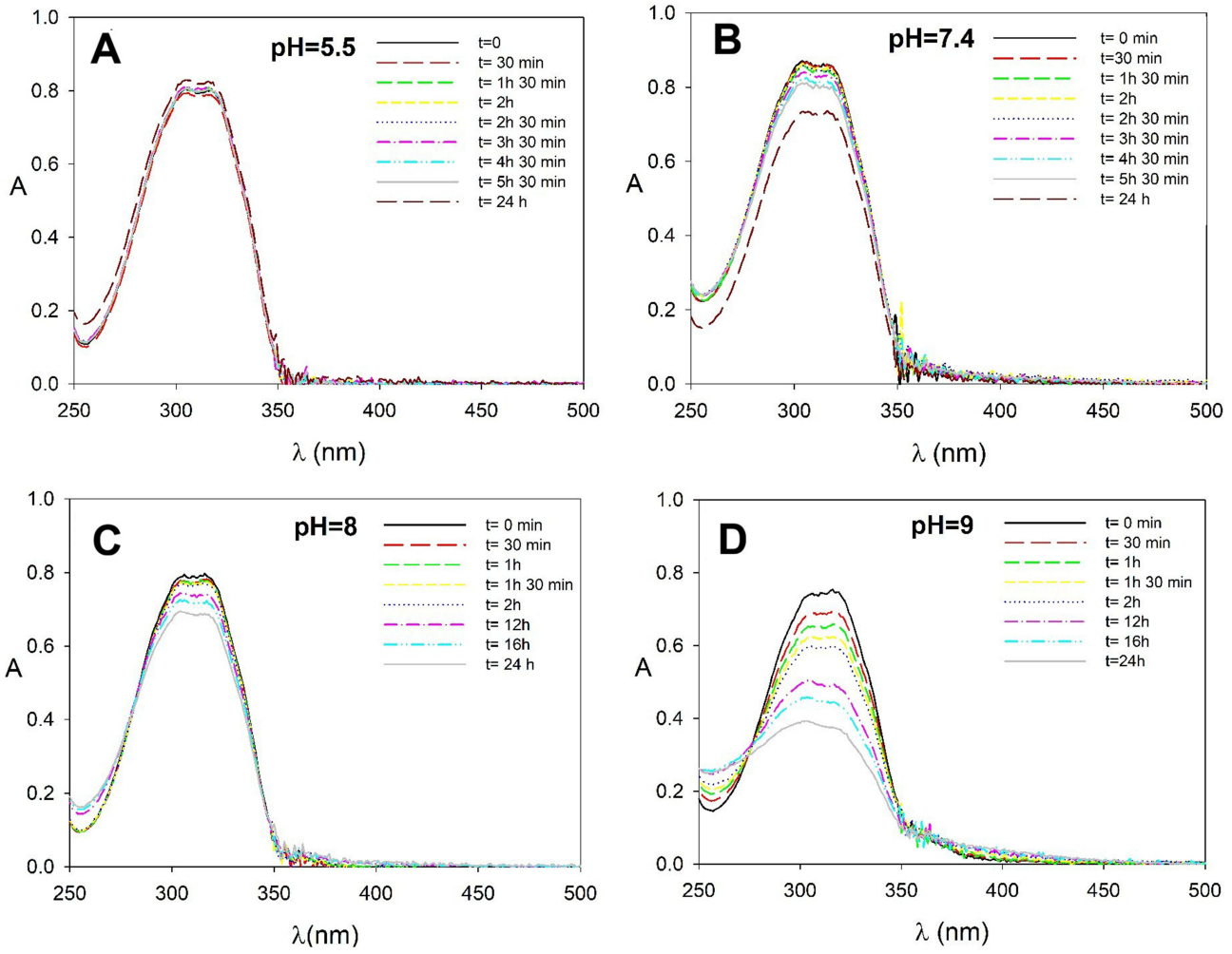

Figure 12 Absorption spectra of a 220 μM RSV solution in calcium acetate 170 mM registered within 24 h, as indicated in the legend, at different pH:5.5 (**A**), 7.4 (**B**), 8 (**C**), 9 (**D**).

liposomes can be ascribed to the amount of RSV in the aqueous core, which increases the osmotic pressure on the hydrophobic bilayer membrane. On the contrary, the decrease in size observed for the DPPC/Chol/TPP3 liposomes can be attributed to the removal of most of the bolaamphiphile during the active loading process of RSV (see Table 1): the final system has a different composition with respect to the one of the liposomes before the loading process, so that the dimensions before and after cannot be compared. This observation was confirmed by the size of the two RSV-liposomes with and without TPP3, which were almost identical after loading. The amount of RSV enclosed in the liposome aqueous phase was evaluated by HPLC after the removal of the unentrapped RSV by dialysis. The EE% was good and the same in the presence and absence of TPP3, in contrast to what happens in the passive loading (Table 1). Prior to column injection for HPLC analysis, the samples were diluted to disrupt the liposomes using a MeOH/water solution (in place of MeOH) and avoid the precipitation of calcium acetate (present in the buffer). However, this dilution did not allow the assessment of the TPP3 concentration in the liposomes. Thus, the amount of TPP3 was evaluated by ^{1}HNMR. NMR analysis revealed that the TPP3 concentration decreased by 80% at the end of the preparation protocol. TPP3 is evidently not firmly anchored to the liposome bilayer membrane if cholesterol was present in the formulation. However, even though the DPPC/Chol/TPP3 liposomes had a lower amount of TPP3 than DPPC/TPP3 and DOPC/TPP3 liposomes (Table 1), they were still able to target mitochondria (see paragraph "Mitochondrial Targeting" and compare Figure 9D with Figure 9B and Figure 10A,B) and entrap RSV.

RSV Passive Loading

In the passive loading method, RSV was added to the lipid mixture (PC/TPP3) in an organic solvent during the preparation of the thin film (RSV/total lipids, 1:8 molar ratio). DOPC and DPPC were chosen to evaluate the influence of the degree of unsaturation of the chains on the physical state of the lipid bilayer membrane and consequently on the trapping efficiency. As for active method, only the 2.5% of TPP3 was used. MLV dispersions obtained by hydration of the mixed film with PBS were subjected to six freeze–thaw and sonication cycles. The sonication process is critical for the high trapping efficiency of RSV in the lipid bilayer because it promotes the disruption of very large aggregates that RSV forms in aqueous solution and fosters RSV inclusion as a monomer in the lipid bilayer. DLS data (Table 1) showed that the obtained liposomes show diameters compatible with those imposed by extrusion. RSV did not significantly affect liposome size or polydispersity, except for DOPC liposomes, where the size decreased in comparison to empty liposome. HPLC evaluation of the amount of RSV enclosed in the liposome bilayer membrane (Table 1) showed that the EE% was the same for the DOPC and DPPC liposomes; thus, the different degree of unsaturation of the phospholipid chains had no influence on the trapping efficiency of RSV. Although EE% decreased in the presence of TPP3, RSV loading was good in all cases, and no size variation was observed. A specifically designed HPLC method to detect the amount of TPP3 in liposomes revealed a partial loss during preparation, larger for DOPC-based (20%) than for DPPC liposomes (8%). This difference may be related to the distinct organization of TPP3 in the two membranes, or to the greater fluidity of the DOPC bilayer membrane, which retains TPP3 less effectively. At the end of the preparation and purification process, RSV-loaded liposomes still contained a fair percentage of the surfactant TPP3 (see Table 1), which was still sufficient for colocalization with mitochondria (Mitochondrial targeting).

RSV Release from Liposomes

To evaluate the influence of the RSV-loading technique on the leakage of RSV from liposomes, a release study at 37°C was performed using the dialysis method for all neutral and cationic liposome formulations prepared by passive and active loading protocols. The DPPC/Chol/TPP3/RSV formulation was excluded because of its instability over time, both after setting the gradient and after resveratrol loading, resulting in irreproducible results. The amount of residual RSV in the liposomes was determined upon time over a period of 20 h. As shown in Figure 13, release of RSV loaded in the internal aqueous cavity of DPPC/Chol liposomes was extremely rapid, with complete leakage observed after 5 h. On the contrary, RSV release rate was markedly lower if RSV was embedded in the lipid bilayer of all the DPPC- and DOPC-based TPP3-liposomes, where leakage between 11–25% was reached after 4 h. In addition, the release rates of DOPC-based liposomes, both in the presence and absence of TPP3, were higher than those of the DPPC-based liposomes. This result could be related to a different localization of RSV in the liposome bilayer.

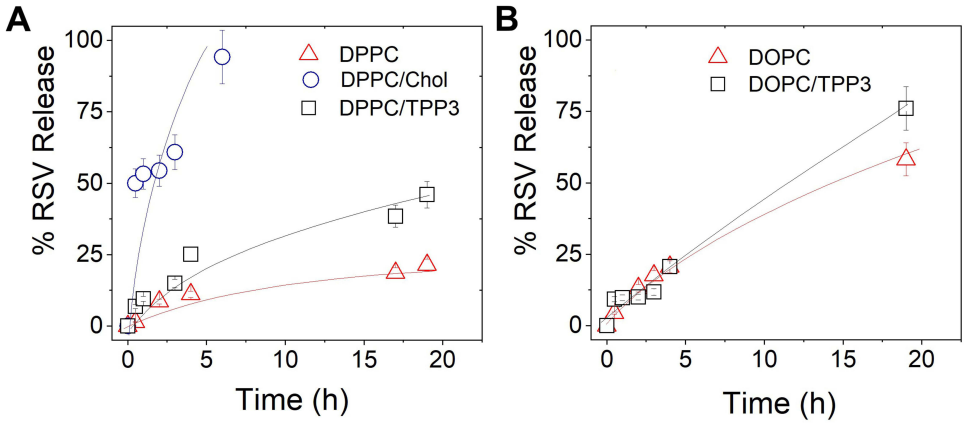

Figure 13 Release of RSV from liposomes over time at 37°C, for the formulations containing DPPC (**A**) and DOPC (**B**), as indicated in the legend. The formulation containing cholesterol was prepared by the active loading technique, all the others by the passive loading technique. The lines only serve as a guide for the eyes. The error associated to % release is the standard deviation of three repeated measurements on three different samples.

https://doi.org/10.2147/IJN.S539303

The results described in this section indicate that: (i) regardless of the loading protocol, optimal loading conditions require RSV/lipid ratios of 1:8 and, in the case of active loading, incubation for 1 h at 45°C; (ii) the inclusion of RSV affects the size or polydispersity of liposomes in different ways, depending on the lipid composition and loading technique; (iii) the EE% by active loading is the same in the presence and absence of TPP3, whereas by passive loading, the EE% decreases in the presence of TPP3; (iv) the RSV release rate from liposomes is lower if RSV is embedded in the lipid bilayer membrane by passive loading and RSV release is faster in the presence of TPP3; and (v) release rate is faster for DOPC-based liposomes with respect to DPPC-based liposomes.

Subcellular Distribution of RSV-Loaded Liposomes

The ability of TPP3-liposomes to deliver RSV (loaded by the passive method technique, as described in the corresponding paragraph "RSV passive loading") to the mitochondria was explored in MDA-MB231 cells. Compared to cells treated with empty liposomes (Figure 14A), the mitochondrial structure appeared better preserved in cells treated with TPP3-liposomes loaded with RSV, which indicated the penetration of RSV into organelles (Figure 14B). This finding opens the possibility of calibrating RSV concentration in liposomal formulations engineered for protective activity in neurodegenerative diseases or for sensitizing activity against drug-resistant tumor cells.

Semiquantitative Analysis of Mitochondrial Targeting

Semi-quantitative colocalization analysis based on Manders' coefficient (Table 4) confirmed that TPP3 significantly enhances mitochondrial targeting in MDA-MB231 cells. Both DOPC/TPP3 and DPPC/TPP3 liposomal formulations exhibited greater colocalization with mitochondria compared to their respective non-TPP3 counterparts (M = 0.977 vs 0.750 for DOPC and M = 0.827 vs 0.611 for DPPC). Among all tested formulations, DOPC/TPP3 liposomes demonstrated the highest degree of mitochondrial overlap (M = 0.977), indicative of rapid cellular uptake and efficient mitochondrial delivery, consistent with the high membrane fluidity characteristic of DOPC-based systems. In contrast, DPPC/TPP3 liposomes showed a slightly reduced colocalization coefficient (M = 0.827), suggesting slower internalization likely attributable to the more rigid, saturated nature of DPPC membranes, which may hinder vesicle uptake.

The incorporation of cholesterol into DPPC/TPP3 liposomes (DPPC/Chol/TPP3) further diminished colocalization efficiency (M = 0.557), presumably due to increased membrane packing density and reduced fusogenicity. Additionally, the inclusion of resveratrol (RSV) in DOPC/TPP3 formulations (DOPC/TPP3/RSV) resulted in decreased mitochondrial colocalization (M = 0.662), potentially due to alterations in the organization of liposome membrane.

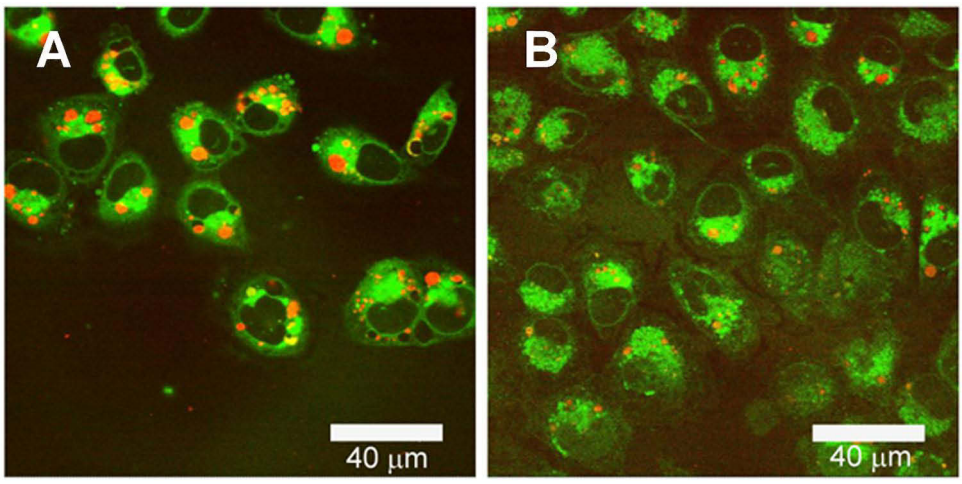

Figure 14 LSCM images of MDA-MB231 cells labelled with MitoTracker probe (green signal), treated for 18 h with DOPC-TPP3 liposomes, empty (**A**) or loaded with RSV by passive method technique (**B**).

Table 4 Semiquantitative Analysis of Mitochondrial Targeting Based on Manders' Coefficient (M)

Liposome Formulation	Manders' M ± SD (Liposomes → Mitochondria)
DOPC	0.75 ± 0.13
DOPC/TPP3	0.98 ± 0.017
DOPC/TPP3/RESV	0.66 ± 0.14
DPPC	0.61 ± 0.13
DPPC/TPP3	0.83 ± 0.098
DPPC/Chol	0.60 ± 0.14
DPPC/Chol/TPP3	0.557 ± 0.071

Notes: Manders' M coefficient quantifies the fraction of liposomes (red fluorescence signal) colocalizing with mitochondria (green fluorescence signal) following 18 hours of treatment in MDA-MB 231 cells.

Collectively, these findings demonstrate that TPP3-functionalized liposomes effectively target mitochondria, with targeting efficiency modulated by lipid composition, cholesterol content, and cargo loading. DOPC-based formulations facilitate rapid mitochondrial delivery, whereas DPPC- and DPPC/Chol-based systems offer more controlled and biocompatible interactions.

Trolox Liposomes

Owing to its high solubility and strong activity both in-vitro and in-vivo, delivering Trolox through a nanovector is not essential. However, encapsulating Trolox in liposomes could improve its stability and biological activity and, most importantly, reduce the required dose.

The structural and physicochemical characteristics of Trolox allow its inclusion in the inner aqueous phase of liposomes via active loading. For this purpose, we explored two different active loading methods: the first exploiting the simple gradient concentration of Trolox and the other relying on the pH gradient across the liposome membrane generated by calcium acetate, as already described for RSV.

Trolox Stability as a Function of pH

Trolox stability was evaluated in the same buffer used for the pH gradient, namely calcium acetate 150 mM at pH 8.2. The main degradation product is Trolox C quinone, a photo-oxidative product that is formed more readily at higher pH. Trolox C quinone absorbs at shorter wavelengths (λ_{max} = 271 nm) and has a much larger molar extinction coefficient than Trolox (Supplementary Material, Figure S5A); thus, it is easily detectable, even in small amounts. Analysis of the UV spectra showed no degradation of Trolox over 24 h at pH 8.2 (Supplementary Material, Figure S5B).

Trolox Active Loading by pH Gradient

As previously observed for RSV, the value of pK_{a1} is crucial for inclusion by the pH gradient method. Trolox should be in neutral form outside the liposomes to easily pass through the lipid bilayer membrane. Once it reaches the internal aqueous cavity, it should be charged to remain entrapped in the aggregate. Moreover, the presence of calcium acetate in the aqueous cavity is required to enhance the retention of Trolox because of the formation of stable complexes with the carboxylate and hydroxyl groups present in Trolox.[82] Since the acid dissociation constant pK_{a1} of Trolox is 3.89, the active loading protocol described in the literature would require a pH of the external phase lower than this value. However, it is reported that Trolox incubated at physiological pH with liposomes can associate with the hydrophobic bilayer membrane by approximately 20–30%,[83] Thus, we tried to trap Trolox in liposomes with an internal pH of 8.2 and external pH of 7.4 (see paragraph "Loading of Trolox in liposomes"), to match physiological pH and ionic strength conditions of the in-vitro test.

DPPC/Chol-TPP3-liposomes exhibited a slightly lower entrapment efficiency and drug/lipid ratio than DPPC/Chol-liposomes (Table 2), indicating that the presence of TPP3 slightly decreased the included Trolox. DLS analysis revealed that inclusion of Trolox promoted an increase in liposome size, probably due to the high drug/lipid ratio, ie the high amount of drug included in each liposome, which, in turn, increased the osmotic pressure on the liposome bilayer membrane. Notably, the encapsulation of Trolox improved its stability. In fact, the UV spectra of Trolox loaded in liposomes (Figure 15) showed only slight degradation after 120 h (A), whereas free Trolox converted to C-quinone to a large extent within 48 h (B).

Trolox Loading by Concentration Gradient

Trolox was added to a dispersion of preformed DPPC/Chol liposomes and incubated for 1 h at 45°C to be loaded by a concentration gradient. The trapping efficiency was 30% (final Trolox/lipids ratio 6:1), which was considerably lower than that obtained using the calcium acetate gradient. This result confirms, on one hand, the ability of Trolox to associate with liposomes, regardless of the pH of the outer phase,[83] and, on the other hand, that a basic internal pH is crucial for achieving stable formulations with higher entrapment efficiency.

Trolox Release from Liposomes

The release of Trolox from the DPPC/Chol and DPPC/Chol/TPP3 liposomes loaded using the pH gradient technique was investigated to evaluate the influence of TPP3 on leakage. The amount of residual Trolox in liposomes was determined over a period of 50 h at 37°C. As is evident from the different trends shown in Figure 16, up to 5 h, Trolox was released at the same rate by the two formulations, reaching in both case ~ 50%. At longer time points, in the presence of TPP3, a faster rate was observed resulting in a complete release after 30 h, whereas for DPPC/Chol liposomes remained ~ 60%. This finding can be correlated with the higher permeability of the DPPC/Chol/TPP3 liposomes.

Conclusion

This paper reports an extensive research aimed at the development of new liposomal formulations containing a triphenylphosphonium (TPP3) bolaamphiphile, which can reach mitochondria and deliver antioxidants with high efficiency.

At first, the most suitable percentage of TPP3 in liposome composition was defined based on biological investigation on empty TPP3-liposomes aimed at selecting the TPP3 percentage which could guarantee targeting to mitochondria and low toxicity at the same time. Such a composition was then selected for loading of antioxidants and further biological investigation on RSV-loaded TPP3-liposomes.

RSV and Trolox were selected for the study, and two loading strategies were examined: passive loading and active loading based on a pH gradient. The impact of lipid formulation (specifically the presence of saturated or unsaturated PC and of cholesterol) on the stability of delivery systems, on the antioxidant entrapment efficiency and on the effect of such factors on the behavior of the drug delivery systems in vitro was investigated.

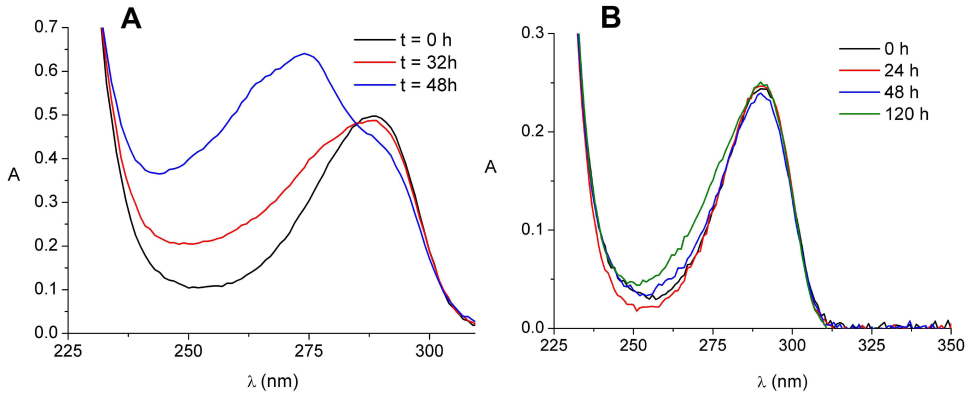

Figure 15 Absorption spectra of Trolox 200 μM in calcium acetate at pH 8.2 (**A**), Trolox loaded in DPPC/Chol liposomes (**B**), at different times.

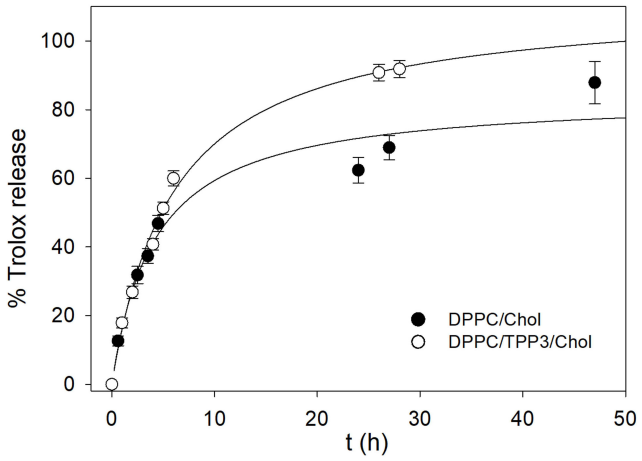

Figure 16 Trolox release (at 37°C) from the liposome formulations prepared by the pH gradient loading technique indicated in the legend. Lines guide the eyes, only. The error associated to % release is the standard deviation of three repeated measurements on three different samples.

The results highlight the crucial role of the composition of liposomes and protocol for antioxidant inclusion in the final properties of the liposomes and their mitochondrial targeting efficiency. The nature of the PC and the thermotropic phase of the hydrophobic bilayer membrane at physiological temperature, the presence of cholesterol, and the cell line are factors that affect the ability of TPP3-liposomes to target the mitochondria. In particular, DOPC/TPP3-liposomes, characterized by a fluid bilayer membrane, show higher cellular uptake in MDA-MB231 than the more rigid DPPC/TPP3-liposomes, and the addition of cholesterol reduces the penetration of liposomes into the cytoplasm and mitochondria.

Most importantly, without any precedent records in the literature, our investigation demonstrated the possibility of loading RSV into the aqueous cavity of liposomes using the pH gradient technique, in addition to the commonly used passive loading method which promotes RSV insertion mainly into the liposome hydrophobic bilayer membrane. Both protocols achieved a high amount of entrapped RSV; however, the release rate showed a marked difference between the two formulations. Liposomes prepared using the pH gradient technique are characterized by an important burst release and complete leakage after 5 h. By contrast, when RSV is embedded in the liposome bilayer membrane, the release rate is markedly lower. This controlled modulation of release could be advantageous depending on the intended application, eg burst release for wound healing or targeted delivery,[84] and prolonged release for sustained antioxidant effect. Similarly, active loading of Trolox enhanced entrapment efficiency and antioxidant stability, highlighting the potential of these liposomal strategies to improve functional performance, although these benefits remain to be confirmed in vivo.

To the best of our knowledge, this is the first report on the inclusion of Trolox in liposomes using the active loading technique, leading to very high entrapment efficiency and improvement of antioxidant stability. Although our findings remain preliminary, Trolox-liposomes, in the non-specific DPPC/Chol formulation or in other target-specific formulations, could potentially find applications in various fields besides subcellular delivery, such as the treatment of glaucoma and retinal damage associated with neurodegeneration, other neurodegenerative diseases[85] and cosmetics production.

At present, our findings are limited to in vitro models. In this regard, the MDA-MB231 human breast cancer cell line, which exhibits multidrug resistance (MDR), seems to be a more suitable model for further studies concerning the application of TPP3-liposomes. In this model, the protective effect of RSV-loaded TPP3 liposomes in preventing mitochondrial collapse is encouraging, although further validation is needed. These preliminary in vitro results pave the way for further studies, aimed at ascertaining the possibility of using RSV incorporated into liposomes as an adjuvant for a protective activity in neurodegenerative diseases, upon careful calibration of the RSV concentration in liposomes. Similarly, RSV-liposomes might have applications as antimicrobial and anti-biofilm agents by impairing pathogen mitochondrial functions[86] and could contribute to sensitizing drug-resistant tumor cells.

Our formulations demonstrate efficient mitochondrial targeting and high antioxidant entrapment in vitro, and represent a starting point for future investigation for the translation to in vivo where factors such as nanoparticle size, surface charge,

https://doi.org/10.2147/IJN.S539303

and liposome membrane composition, which can affect biodistribution, clearance, and off-target interactions should be considered, as well as long-term safety, immunogenicity, to cite only few aspects. Addressing these aspects will be essential for the successful translation of RSV and Trolox liposomes into clinical applications. In addition, the feasibility of scaling up liposome production under GMP standards and thorough preclinical safety evaluations, including immunogenicity and in vivo toxicity, will be important considerations for the clinical translation of RSV and Trolox liposomes.

Abbreviations

ROS, Reactive Oxygen Species; TPP, triphenylphosphonium bolaamphiphile; DQA, dequalinium chloride; TPP3, bolaamphiphile with a spacer of 20 methylene units: Eicosane-1,20-diylbis(triphenylphosphonium) bromide; triphenylphosphonium; DPPC, 1,2-dipalmitoyl-sn-glycero-3-phosphocholine; DOPC, 1,2-dioleoyl-sn-glycero-3-phosphocholine; PC, phosphocholine; MDR, multi-drug resistance; HER-2, estrogen receptor; TNBC, triple negative breast cancer; RSV, trans-resveratrol; DLS, Dynamic light scattering; DELS, Dynamic dielectrophoretic light scattering; LSCM, Laser scanning confocal microscopy; MTT, 3-(4,5-dimethylthiazol-2-yl)-2,5-diphenyltetrazolium bromide; STPP Stearyltriphenyl- phosphonium, DPX, *p*-xylene-bis-pyridinium bromide; DMEM, Dulbecco's Modified Eagle's Medium; FBS, Fetal Bovine Serum; PBS, phosphate buffer saline; HEPES, N-2-hydroxyethylpiperazine-N′-2-ethanesulfonic acid; Chol, cholesterol; T_M, Transition temperature; 16:0 Rhod-PE, 1,2-dipalmitoyl-sn-glycero-3-phosphoethanolamine-N-(lissamine rhodamine B sulfonyl) (ammonium salt); 18:1 Rhod PE, 1,2-dioleoyl-sn-glycero-3-phosphoethanolamine-N-(lissamine rhodamine B sulfonyl) (ammonium salt); MLV, multilamellar vesicles; PDI, polidispersity index; TSB, trans-stilbene; SD, standard deviation; HPLC, High performance liquid cromatography; ^{1}H NMR, Hydrogen nuclear magnetic resonance; NNLS, non-negative least squares; HCl, hydrochloric acid; NaOH, sodium hydroxide; DMSO, dimethyl sulfoxide; EtOH, ethanol; MeOH, methanol; $HClO_4$, perchloric acid; Me_4NOH, Tetramethylammonium hydroxide; TMRM, tetramethyl-Rhodamine methyl ester.

Acknowledgments

S. S. and C. B. acknowledge financial support under the National Recovery and Resilience Plan (NRRP), Mission 4, Component 2, Investment 1.1, Call for tender No. 104 published on 2.2.2022 by the Italian Ministry of University and Research (MUR), funded by the European Union – NextGenerationEU– Project Title "Biomimetic antimicrobial vesicle-like nanoarchitectures for multi-drug-resistant bacteria—Believe" – CUP B53D23013710006 and from Mission 4, Component 2, Investment 1.3, Call for tender No. 341 published on 15.3.2022 by the Italian Ministry of University and Research (MUR), funded by the European Union - NextGenerationEU – Project "One Health Basic and Translational Research Actions addressing Unmet Needs on Emerging Infectious Diseases—INFACT- PE00000007" – CUP B53C20040570005.

Author Contributions

All authors made a significant contribution to the work reported, whether that is in the conception, study design, execution, acquisition of data, analysis and interpretation, or in all these areas; took part in drafting, revising or critically reviewing the article; gave final approval of the version to be published; have agreed on the journal to which the article has been submitted; and agree to be accountable for all aspects of the work.

Disclosure

The author(s) report no conflicts of interest in this work.

References

1. Baines CP. Role of the mitochondrion in programmed necrosis. *Front Physiol*. 2010;1:156. doi:10.3389/fphys.2010.00156
2. Gruber J, Fong S, Chen CB, et al. Mitochondria-targeted antioxidants and metabolic modulators as pharmacological interventions to slow ageing. *Biotechnol Adv*. 2013;31:563–592. doi:10.1016/j.biotechadv.2012.09.005
3. Buchke S, Sharma M, Bora A, et al. Mitochondria-targeted, nanoparticle-based drug-delivery systems: therapeutics for mitochondrial disorders. *Life*. 2022;12:657. doi:10.3390/life12050657

4. Xu J, Shamul JG, Kwizera EA, et al. Recent advancements in mitochondria-targeted nanoparticle drug delivery for cancer therapy. *Nanomaterials*. 2022;12:743. doi:10.3390/nano12050743
5. Khan T, Waseem R, Zehra Z, et al. Mitochondrial dysfunction: pathophysiology and mitochondria-targeted drug delivery approaches. *Pharmaceutics*. 2022;14:2657. doi:10.3390/pharmaceutics14122657
6. Wongrakpanich A, Geary SM, Joiner MLA, et al. Mitochondria-targeting particles. *Nanomedicine*. 2014;9:2531–2543. doi:10.2217/nnm.14.161
7. Katayama T, Kinugawa S, Takada S, et al. A mitochondrial delivery system using liposome-based nanocarriers that target myoblast cells. *Mitochondrion*. 2019;49:66–72. doi:10.1016/j.mito.2019.07.005
8. Benien P, Solomon MA, Nguyen P, et al. Hydrophobized triphenylphosphonium derivatives for the preparation of mitochondriotropic liposomes: choice of hydrophobic anchor influences cytotoxicity but not mitochondriotropic effect. *J Liposome Res*. 2016;26:21–27. doi:10.3109/08982104.2015.1022557
9. Xu Y, Wang S, Chan HF, et al. Triphenylphosphonium-modified poly(ethylene glycol)-poly(ε-caprolactone) micelles for mitochondria- targeted gambogic acid delivery. *Int J Pharm*. 2017;522:21–33. doi:10.1016/j.ijpharm.2017.01.064
10. Biswas S, Dodwadkar NS, Deshpande PP, Torchilin VP. Liposomes loaded with paclitaxel and modified with novel triphenylphosphonium-PEG-PE conjugate possess low toxicity, target mitochondria and demonstrate enhanced antitumor effects in vitro and in vivo. *J Control Release*. 2012;159:393–402. doi:10.1016/j.jconrel.2012.01.009
11. Kuznetsova DA, Vasileva LA, Gaynanova GA, et al. Comparative study of cationic liposomes modified with triphenylphosphonium and imidazolium surfactants for mitochondrial delivery. *J Mol Liq*. 2021;330:115703. doi:10.1016/j.molliq.2021.115703
12. Zhou J, Zhao WY, Ma X, et al. The anticancer efficacy of paclitaxel liposomes modified with mitochondrial targeting conjugate in resistant lung cancer. *Biomaterials*. 2013;34:3626–3638. doi:10.1016/j.biomaterials.2013.01.078
13. Ceccacci F, Sennato S, Rossi E, et al. Aggregation behaviour of triphenylphosphonium bolaamphiphiles. *J Colloid Interface Sci*. 2018;531:451–462. doi:10.1016/j.jcis.2018.07.067
14. Ceccacci F, Sennato S, Rossi E. Chapter synthesis and characterization of mitochondria-targeted triphenyltriphenylphosphonium bolaamphiphiles. In: Weissig V, Edeas M, editors. *Mitochondrial Medicine: Methods in Molecular Biology*. Vol. 1, 2nd ed. Humana Press; 2021:27–48.
15. Sondag GR, Salihoglu S, Lababidi SL, et al. Osteoactivin induces transdifferentiation of C2C12 myoblasts into osteoblasts. *J Cell Physiol*. 2014;229:955–966. doi:10.1002/jcp.24512
16. Nedeljkovic M, Damjanovic A. Mechanisms of chemotherapy resistance in triplenegative breast cancer—how we can rise to the challenge. *Cells*. 2019;8:957. doi:10.3390/cells8090957
17. Jiang L, Li L, He X, et al. Overcoming drug-resistant lung cancer by paclitaxel loaded dual-functional liposomes with mitochondria targeting and pH-response. *Biomaterials*. 2015;52:126–139. doi:10.1016/j.biomaterials.2015.02.004
18. Fernandes GFS, Silva GDB, Pavan AR, et al. Epigenetic regulatory mechanisms induced by resveratrol. *Nutrients*. 2017;9:1201. doi:10.3390/nu9111201
19. Kaminski J, Lançon A, Aires V, et al. Resveratrol initiates differentiation of mouse skeletal muscle-derived C2C12 myoblasts. *Biochem Pharmacol*. 2012;84:1251–1259. doi:10.1016/j.bcp.2012.08.023
20. Baxter RA. Anti-aging properties of resveratrol: review and report of a potent new antioxidant skin care formulation. *J Cosmet Dermatol*. 2008;7:2–7. doi:10.1111/j.1473-2165.2008.00354.x
21. Jang M, Cai L, Udeani GO, et al. Cancer chemopreventive activity of resveratrol, a natural product derived from grapes. *Science*. 1997;275:218–220. doi:10.1126/science.275.5297.218
22. Sareen D, Van Ginkel PR, Takach JC, et al. Mitochondria as the primary target of resveratrol-induced apoptosis in human retinoblastoma cells. *Invest Ophthalmol Visual Sci*. 2006;47:3708–3716. doi:10.1167/iovs.06-0119
23. Chen Z, Jin K, Gao L, et al. Anti-tumor effects of bakuchiol, an analogue of resveratrol, on human lung adenocarcinoma A549 cell line. *Eur J Pharmacol*. 2010;643:170–179. doi:10.1016/j.ejphar.2010.06.025
24. Shukla Y, Singh R. Resveratrol and cellular mechanisms of cancer prevention. *Ann N Y Acad Sci*. 2011;1215:1–8. doi:10.1111/j.1749-6632.2010.05870.x
25. Dean RT, Hunt JV, Grant AJ, et al. Free radical damage to proteins: the influence of the relative localization of radical generation, antioxidants, and target proteins. *Free Radic Biol Med*. 1991;11:161–168. doi:10.1016/0891-5849(91)90167-2
26. Neužil J, Gebicki J, Stocker R. Radical-induced chain oxidation of proteins and its inhibition by chain-breaking antioxidants. *Biochem J*. 1993;293:601–606. doi:10.1042/bj2930601
27. Giulivi C, Cadenas E. Inhibition of protein radical reactions of ferrylmyoglobin by the water-soluble analog of vitamin E, Trolox C. *Arch Biochem Biophys*. 1993;303:152–158. doi:10.1006/abbi.1993.1266
28. Nakamura M. One-electron oxidation of Trolox C and vitamin E by peroxidases. *J Biochem*. 1991;110:595–597. doi:10.1093/oxfordjournals.jbchem.a123625
29. Laughton MJ, Evans PJ, Moroney MA, et al. Inhibition of mammalian 5-lipoxygenase and cyclo-oxygenase by flavonoids and phenolic dietary additives: relationship to antioxidant activity and to iron ion-reducing ability. *Biochem Pharmacol*. 1991;42:1673–1681. doi:10.1016/0006-2952(91)90501-U
30. Phoenix J, Edwards R, Jackson MJ. Inhibition of Ca2+-induced cytosolic enzyme efflux from skeletal muscle by vitamin E and related compounds. *Biochem J*. 1989;257:207–213. doi:10.1042/bj2570207
31. Smith CE, Stack MS, Johnson DA. Ozone effects on inhibitors of human neutrophil proteinases. *Arch Biochem Biophys*. 1987;253:146–155. doi:10.1016/0003-9861(87)90647-3
32. Crivello JF. Interaction of bovine renal mitochondrial cytochrome P-450 with antioxidants. *Arch Biochem Biophys*. 1986;248:551–561. doi:10.1016/0003-9861(86)90508-4
33. Ramassamy C, Naudin B, Christen Y, et al. Prevention by Ginkgo biloba extract (EGb 761) and trolox C of the decrease in synaptosomal dopamine or serotonin uptake following incubation. *Biochem Pharmacol*. 1992;44:2395–2401. doi:10.1016/0006-2952(92)90685-C
34. Britt SG, Chiu VW, Redpath GT, Vandenberg SR. Elimination of ascorbic acid-induced membrane lipid peroxidation and serotonin receptor loss by Trolox-C, a water soluble analogue of vitamin E. *J Recept Res*. 1992;12:181–200. doi:10.3109/10799899209074791
35. Wu T-W, Hashimoto N, Wu J, et al. The cytoprotective effect of Trolox demonstrated with three types of human cells. *Biochem Cell Biol*. 1990;68:1189–1194. doi:10.1139/o90-176

36. Persoon-Rothert M, Egas-Kenniphaas J, Van der Valk-Kokshoorn E, et al. Prevention of cumene hydroperoxide induced oxidative stress in cultured neonatal rat myocytes by scavengers and enzyme inhibitors. *J Mol Cell Cardiol*. 1990;22:1147–1155. doi:10.1016/0022-2828(90)90078-G
37. Casini A, Pompella A, Comporti M. Liver glutathione depletion induced by bromobenzene, iodobenzene, and diethylmaleate poisoning and its relation to lipid peroxidation and necrosis. *Am J Pathol*. 1985;118:225.
38. Massey KD, Burton KP. Free radical damage in neonatal rat cardiac myocyte cultures: effects of α-tocopherol, Trolox, and phytol. *Free Radic Biol Med*. 1990;8:449–458. doi:10.1016/0891-5849(90)90058-Q
39. Suttorp N, Toepfer W, Roka L. Antioxidant defense mechanisms of endothelial cells: glutathione redox cycle versus catalase. *Am J Physiol Cell Physiol*. 1986;251:C671–C680. doi:10.1152/ajpcell.1986.251.5.C671
40. Mayer L, Hope M, Cullis P. Vesicles of variable sizes produced by a rapid extrusion procedure. *Biochim Biophys Acta Biomembranes*. 1986;858:161–168. doi:10.1016/0005-2736(86)90302-0
41. Koppel DE. Analysis of macromolecular polydispersity in intensity correlation spectroscopy: the method of cumulants. *J Chem Phys*. 1972;57:4814–4820. doi:10.1063/1.1678153
42. Lawson CL, Hanson RJ. *Solving Least Squares Problems*. SIAM; 1995.
43. Tscharnuter WW. Mobility measurements by phase analysis. *Appl Opt*. 2001;24:3995–4003. doi:10.1364/AO.40.003995
44. Michel N, Fabiano AS, Polidori A, et al. Determination of phase transition temperatures of lipids by light scattering. *Chem Phys Lipids*. 2006;139:11–19. doi:10.1016/j.chemphyslip.2005.09.003
45. Salvio R, Cacciapaglia R, Mandolini L, et al. Diguanidinocalix [4] arenes as effective and selective catalysts of the cleavage of diribonucleoside monophosphates. *RSC Adv*. 2014;4:34412–34416. doi:10.1039/C4RA05751A
46. Salvio R, Volpi S, Cacciapaglia R, et al. Phosphoryl transfer processes promoted by a trifunctional calix [4] arene inspired by DNA topoisomerase I. *J Org Chem*. 2016;81:9012–9019. doi:10.1021/acs.joc.6b01643
47. Salvio R, Moliterno M, Caramelli D, et al. Kinetic resolution of phosphoric diester by Cinchona alkaloid derivatives provided with a guanidinium unit. *Catal Sci Technol*. 2016;6:2280–2288. doi:10.1039/C5CY01208B
48. Alderighi L, Gans P, Ienco A, et al. Hyperquad simulation and speciation (HySS): a utility program for the investigation of equilibria involving soluble and partially soluble species. *Coord Chem Rev*. 1999;184:311–318. doi:10.1016/S0010-8545(98)00260-4
49. Torchilin V, Weissig V. *Liposomes: A Practical Approach*. Oxford University Press; 2003.
50. Clerc S, Barenholz Y. Loading of amphipathic weak acids into liposomes in response to transmembrane calcium acetate gradients. *Biochim Biophys Acta Biomembranes*. 1995;1240:257–265. doi:10.1016/0005-2736(95)00214-6
51. Bonechi C, Martini S, Ciani L, et al. Using liposomes as carriers for polyphenolic compounds: the case of trans-resveratrol. *PLoS One*. 2012;7:1–11. doi:10.1371/journal.pone.0041438
52. Sieuwerts AM, Klijn JG, Peters HA, Foekens JA. The MTT tetrazolium salt assay scrutinized: how to use this assay reliably to measure metabolite activity of cell cultures in vitro for the assessment of growth characteristics, IC_{50}-values and cell survival. *Eur J Clin Chem Clin Biochem*. 1995;33:813–823. doi:10.1515/cclm.1995.33.11.813
53. Dunn KW, Kamocka MM, McDonald JH. A practical guide to evaluating colocalization in biological microscopy. *Am J Physiol Cell Physiol*. 2011;300:C723–42. doi:10.1152/ajpcell.00462.2010
54. Mamusa M, Salvatore A, Berti D. Structural modifications of DPPC bilayers upon inclusion of an antibacterial cationic bolaamphiphile. *Langmuir*. 2018;34:8952–8961. doi:10.1021/acs.langmuir.8b01689
55. Gu Q, Zou A, Yuan C, Guo R. Effects of a bolaamphiphile on the structure of phosphatidylcholine liposomes. *J Colloid Interface Sci*. 2003;266:442–447. doi:10.1016/S0021-9797(03)00649-0
56. Simonis B, Vignone D, Paz OG, et al. Transport of cationic liposomes in a human blood brain barrier model: role of the stereochemistry of the gemini amphiphile on liposome biological features. *J Colloid Interface Sci*. 2022;627:283–298. doi:10.1016/j.jcis.2022.07.025
57. Brownholland DP, Longo GS, Struts AV, et al. Phase separation in binary mixtures of bipolar and monopolar lipid dispersions revealed by 2H NMR spectroscopy, small angle x-ray scattering, and molecular theory. *Biophys J*. 2009;97:2700–2709. doi:10.1016/j.bpj.2009.06.058
58. Haran G, Cohen R, Bar LK. Barenholz Y Transmembrane ammonium sulfate gradients in liposomes produce efficient and stable entrapment of amphipathic weak bases. *Biochim Biophys Acta Biomembranes*. 1993;1151:201–215. doi:10.1016/0005-2736(93)90105-9
59. Giuliani C, Altieri B, Bombelli C, et al. Remote loading of aloe emodin in gemini-based cationic liposomes. *Langmuir*. 2015;31:76–82. doi:10.1021/la5038074
60. Creed S, McKenzie M. Measurement of mitochondrial membrane potential with the fluorescent dye Tetramethylrhodamine Methyl Ester (TMRM). *Methods Mol Biol*. 2019;1928:69–76.
61. Prates Mori M, Lozoya OA, Brooks AM, et al. Mitochondrial membrane hyperpolarization modulates nuclear DNA methylation and gene expression through phospholipid remodeling. *Nat Commun*. 2025;16:4029. doi:10.1038/s41467-025-59427-5
62. Warnes G. Flow cytometric detection of hyper-polarized mitochondria in regulated and accidental cell death processes. *Apoptosis*. 2020;25:548–557. doi:10.1007/s10495-020-01613-5
63. Parisi K, McKenna JA, Lowe R, et al. Hyperpolarisation of mitochondrial membranes is a critical component of the antifungal mechanism of the plant defensin, Ppdef1. *J Fungi*. 2024;10(1):54. doi:10.3390/jof10010054
64. Amri A, Chaumeil J, Sfar S, Charrueau C. Administration of resveratrol: what formulation solutions to bioavailability limitations? *J Control Release*. 2012;158:182–193. doi:10.1016/j.jconrel.2011.09.083
65. Intagliata S, Modica MN, Santagati LM, Montenegro L. Strategies to improve resveratrol systemic and topical bioavailability: an update. *Antioxidants*. 2019;8:244. doi:10.3390/antiox8080244
66. Bohara RA, Tabassum N, Singh MP, et al. Recent overview of resveratrol's beneficial effects and its nano-delivery systems. *Molecules*. 2022;27:5154. doi:10.3390/molecules27165154
67. Wang -X-X, Li Y-B, Yao H-J, et al. The use of mitochondrial targeting resveratrol liposomes modified with a dequalinium polyethylene glycol-distearoylphosphatidyl ethanolamine conjugate to induce apoptosis in resistant lung cancer cells. *Biomaterials*. 2011;32:5673–5687. doi:10.1016/j.biomaterials.2011.04.029
68. Meng J, Guo F, Xu H, et al. Combination therapy using co-encapsulated resveratrol and paclitaxel in liposomes for drug resistance reversal in breast cancer cells in vivo. *Sci Rep*. 2016;6:22390. doi:10.1038/srep22390

69. Tsujioka T, Sasaki D, Takeda A, et al. Resveratrol-encapsulated mitochondria-targeting liposome enhances mitochondrial respiratory capacity in myocardial cells. *Int J Mol Sci*. 2021;23:112. doi:10.3390/ijms23010112
70. Kang JH, Ko YT. Enhanced subcellular trafficking of resveratrol using mitochondriotropic liposomes in cancer cells. *Pharmaceutics*. 2019;11:423. doi:10.3390/pharmaceutics11080423
71. Catania A, Barrajón-Catalán E, Nicolosi S, et al. Immunoliposome encapsulation increases cytotoxic activity and selectivity of curcumin and resveratrol against HER2 overexpressing human breast cancer cells. *Breast Cancer Res Treat*. 2013;141:55–65. doi:10.1007/s10549-013-2667-y
72. Caddeo C, Pucci L, Gabriele M, et al. Stability, biocompatibility and antioxidant activity of PEG-modified liposomes containing resveratrol. *Int J Pharm*. 2018;538:40–47. doi:10.1016/j.ijpharm.2017.12.047
73. Jhaveri A, Deshpande P, Pattni B, et al. Transferrin-targeted, resveratrol-loaded liposomes for the treatment of glioblastoma. *J Control Release*. 2018;277:89–101. doi:10.1016/j.jconrel.2018.03.006
74. Kim SH, Adhikari BB, Cruz S, et al. Targeted intracellular delivery of resveratrol to glioblastoma cells using apolipoprotein E-containing reconstituted HDL as a nanovehicle. *PLoS One*. 2015;10:e0135130. doi:10.1371/journal.pone.0135130
75. Trela BC, Waterhouse AL. Resveratrol: isomeric molar absorptivities and stability. *J Agric Food Chem*. 1996;44:1253–1257. doi:10.1021/jf9504576
76. Lopez-Nicolas JM, Garcia-Carmona F. Aggregation state and pK_a values of (E)-resveratrol as determined by fluorescence spectroscopy and UV-visible absorption. *J Agric Food Chem*. 2008;56:7600–7605. doi:10.1021/jf800843e
77. Cao J, Chen GH, Du YS, et al. Determination of dissociation constants of resveratrol and polydatin by capillary zone electrophoresis. *J Liquid Chromatogr Related Technol*. 2006;29:1457–1463. doi:10.1080/10826070600674877
78. Takagai Y, Kubota T, Kobayashi H, et al. Adsorption and desorption properties of trans-resveratrol on cellulose cotton. *Anal Sci*. 2005;21:183–186. doi:10.2116/analsci.21.183
79. Haynes WM. *CRC Handbook of Chemistry and Physics*. 90th ed.; Ed. Lide DR. Boca Raton (FL): CRC press; 2010.
80. Matsuura BS, Keylor MH, Li B, et al. A scalable biomimetic synthesis of resveratrol dimers and systematic evaluation of their antioxidant activities. *Angew Chem*. 2015;127:3825–3828. doi:10.1002/ange.201409773
81. Shang Y-J, Qian Y-P, Liu XD, et al. Radical-scavenging activity and mechanism of resveratrol-oriented analogues: influence of the solvent, radical, and substitution. *J Org Chem*. 2009;74:5025–5031. doi:10.1021/jo9007095
82. Cannan RK, Kibrick A. Complex formation between carboxylic acids and divalent metal cations. *J Am Chem Soc*. 1938;60:2314–2320. doi:10.1021/ja01277a012
83. Barclay LRC, Baskin KA, Dakin KA, et al. The antioxidant activities of phenolic antioxidants in free radical peroxidation of phospholipid membranes. *Can J Chem*. 1990;68:2258–2269. doi:10.1139/v90-348
84. Huang X, Brazel CS. On the importance and mechanisms of burst release in matrix-controlled drug delivery systems. *J Control Release*. 2001;73:121–136. doi:10.1016/S0168-3659(01)00248-6
85. Upreti S, Ghosh MP. Chapter 9: trolox assisted inhibition of glutamate excitotoxicity-mediated degeneration in retina. In: *Contemporary Medical Biotechnology Research for Human Health*. Academic Press; 2022.
86. Valderrama V, Sánchez P, Delso M, et al. Gallic acid and triphenylphosphonium derivatives TPP+-C10 and TPP+-C12 inhibit mitochondrial function in Candida albicans exerting antifungal and antibiofilm effects. *J Appl Microbiol*. 2024;135:lxad316. doi:10.1093/jambio/lxad316